Cellulose reinforced polymer composites and nanocomposites: a critical review

Chuanwei Miao & Wadood Y. Hamad

Cellulose

ISSN 0969-0239

Cellulose
DOI 10.1007/s10570-013-0007-3

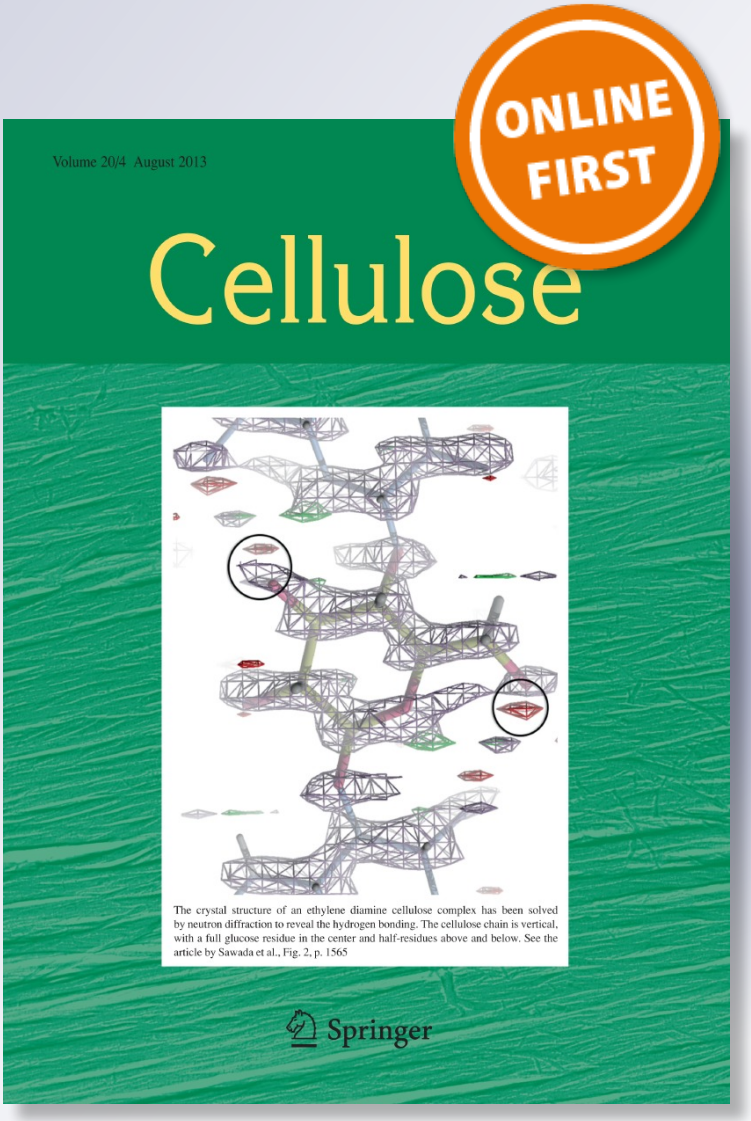

Springer

Cellulose
DOI 10.1007/s10570-013-0007-3

REVIEW PAPER

Cellulose reinforced polymer composites and nanocomposites: a critical review

Chuanwei Miao · Wadood Y. Hamad

Received: 10 December 2012 / Accepted: 22 July 2013

Abstract This review provides a critical assessment of the use of cellulosic materials for reinforcement in polymer composites. The review focuses on structure–property interrelationships and the compatibilization of cellulosic materials for optimal performance of the resulting composite materials. Optimal material and physical properties are characterized on the basis of the reinforcement's physical dimension and the nature of the interface between reinforcement and matrix. We explore how very different cellulosic materials—bacterial, microcrystalline, microfibrillated or nanocrystalline—can cause distinctly different reinforcment.

Keywords Cellulose · Composites · Nanomaterials · Polymer · Renewable

Introduction

Composites are a class of materials that comprise two or more distinct components with significantly different physical and/or chemical properties. The resulting composite can have enhanced mechanical performance (relative to that of the matrix), and/or new functionalities (e.g., barrier performance). Usually, a composite contains a strong and stiff component, the reinforcement, embedded in a softer (relative to the reinforcement) constituent, the matrix. In such a way, the composite has strength properties between those of the reinforcement and the matrix (Fig. 1).

Many natural materials are composites. For example, wood fibres consist of cellulose microfibrils embedded in an amorphous matrix of lignin and hemicellulose; bone and teeth are composed of inorganic crystals in a matrix of collagen. Composites can be classified into 3 categories in terms of the type of matrix used: (1) polymer matrix composites (PMCs), (2) metal matrix composites (MMCs) and (3) ceramic matrix composites (CMCs). The majority of artificial composites use thermosetting resins and polymers, like unsaturated polyester (Vilay et al. 2008), phenolic resin (Zarate et al. 2008), epoxy resin (Zhou et al. 2006) and rubber (Setua and De 1984), and thermoplastic polymers, such as poly(ethylene) (Lu et al. 2007), poly(propylene) (Rezaei et al. 2008), poly(vinyl chloride) (Chazeau et al. 1999) and poly(ethylene oxide) (Chen and Tsubokawa 2000). Due to growing concerns over sustainability and environmental protection, efforts have been made to produce biodegradable polymer composites based on, for example, poly(lactic acid) (Bondeson and Oksman 2007a, b; Oksman et al. 2006), poly(hydroxybutyrate) (Singh et al. 2008), starch (Kvien et al. 2007; Angles and Dufresne 2001), cellulose (Gindl and Keckes 2005; Nishino et al. 2004), and poly(hydroxyoctanoate) (Dubief et al. 1999; Dufresne 2000). Composite

C. Miao · W. Y. Hamad (✉)
FPInnovations, 3800 Wesbrook Mall, Vancouver, BC V6S 2L9, Canada
e-mail: wadood.hamad@fpinnovations.ca

Published online: 04 August 2013

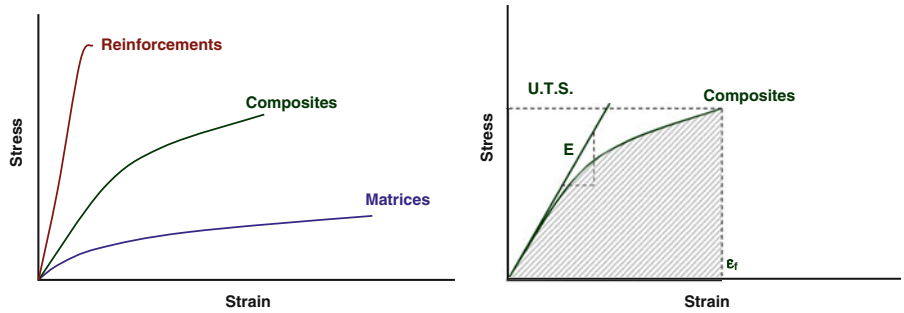

Fig. 1 Schematic illustrations of the strength properties of reinforcement, matrices and composites (on the *left*) and the physical properties obtained from a stress–strain curve (on the *right*). Here, UTS = ultimate tensile strength; ε_f = strain at failure; E = modulus of elasticity; toughness = the shadow area under stress–strain curve (includes both elastic and plastic contributions)

materials can use the characteristics of the reinforcement and the matrix to achieve pronounced property improvements, particularly, strength. A typical example is glass-reinforced plastics (GRP), which are made of fibreglass and a thermosetting plastic, most often polyester. Glass fibers have high tensile strength, but no resistance to compression. On the other hand, the plastic resin, polyester, is strong under compressive loading and relatively weak in tensile strength. GRP has superior properties in both compressive and tensile strengths. Compared to steel, GRP has good strength, light weight and resistance to chemicals, and it is thus widely used in aircraft, automobiles, boats, storage tanks, construction, piping, etc. Compared to polymer matrix composites, strength improvements in metal matrix composites via the introduction of reinforcements are not typically the objective, rather other physical improvements, such as high-temperature performance and tribological properties are often of interest. With regard to ceramic matrix composites, the primary goal of the reinforcement is to improve the toughness of the matrix ceramic, which is otherwise brittle.

Reinforcements in composites can be classified structurally as: woven, continuous fibres, short fibres and particles, or, morphologically, as macroscopic, microscopic or nanoscopic based on their physical size. Conventional composites use macroscopic cloth, or fibers, or microscopic short fibres as the reinforcements. The reinforcement in a nanocomposite has at least one dimension in the nanometer range, usually less than 100 nm. The addition of the nano-reinforcements can improve the properties of composites because of the high specific surface area of the reinforcement (hundreds m^2/g of materials). Some examples of reinforcements are listed in Table 1.

The strength of polymer composites depends on 4 factors: (1) the properties of the matrix; (2) the properties of the reinforcement; (3) the reinforcement–matrix compatibility and interaction; and (4) the dispersion of the reinforcement in the matrix for short fiber- or particle-reinforced systems. In classical composites, interfacial interactions are required to bond them together. The most common interactions are van der Waals forces, while others include: electrostatic attractions, chemical bonds, molecular entanglement and mechanical interlocking. Processing conditions play an important role in determining the composite properties. Two different examples are offered. (1) Freshly drawn glass fibers have high strength, whereas the strength decreases if the fibers are exposed to humid air when water is adsorbed onto the fibers, or the fiber surfaces become damaged due to rubbing action during processing. To minimize this type of influence, glass fibers are usually sized using an emulsified aqueous polymer solution (Hull and Clyne 1996). (2) The processing temperature of lignocellulosic materials is restricted to about 200 °C as these materials start to degrade near 230 °C, which limits the type of thermoplastics that can be used in composites manufacture (Hamad 2002).

This review summarizes advances in the use of cellulosic reinforcements in polymer composites and nanocomposites. The interest to use cellulosic materials as load bearing constituents in composite materials is increasing because they are inexpensive, recyclable, a renewable resource, and have high strength-to-weight ratio.

Table 1 Examples of common types of reinforcement (Hull and Clyne 1996; Samir et al. 2004c; Fedullo et al. 2007; Kashiwagi et al. 2004; Njuguna et al. 2007)

Types	d (μm)	L (μm)	Examples
Monofilaments (large-diameter single fibers)	100–150	∞	SiC, boron
Multifilaments (tows or woven rovings with up to 14,000 fibers per strand)	7–30	∞	Carbon, glass, aramid fibres, FP™ alumina
Short fibers (staple fibers aggregated into blankets, tapes, wools, etc.)	1–10	50–5,000	Saffil™, Kaowool™, Fiberfax™
Micro-whiskers (fine single crystals in loose aggregates)	0.1–1	5–100	SiC, Al_2O_3
Micro-particulate (powders)	5–20	5–20	SiC, Al_2O_3, B_4C, microcrystalline cellulose
Nano-reinforcements (fibers, whiskers, platelets, particles)	0.002–0.1	0.1–2 (fibers and whiskers) <0.1 (particles)	Silicate clays, carbon nanotubes, cellulose nanocrystals

Cellulose fiber reinforced composites

Cellulose is the most abundant natural organic compound, comprising at least one-third of the vegetable matter in the world. It is a polysaccharide containing a linear chain with hundreds to thousands of β-1,4 linked D-glucose units (Fig. 2). Due to the presence of multiple hydroxyl groups on cellulose, numerous hydrogen bonds are formed between the hydrogen and oxygen molecules, intra- and inter-molecularly. As such, cellulose chains are held firmly by these forces to form microfibrils with very high tensile strength. For a perfect crystal of cellulose, the theoretically predicted elastic modulus and tensile strength is 150 and 10 GPa, respectively (Sakurada and Nukushina 1962), which are comparable to aramid fibers (Kevlar).

Cellulosic materials have several advantages. Cellulose is:

1. Biodegradable and CO_2 neutral;
2. An abundant resource—a wide variety of fibers are available all over the world;
3. Formed using solar energy;
4. Low cost;

Cellulose has:

1. High specific strength and modulus—the maximum macroscopic Young's modulus of natural plant cellulose fibers is 128 GPa (Page et al. 1971)
2. High sound damping performance due to the hollow structure of fibers;
3. Low density; and
4. A relatively reactive surface, which can be used for surface modification.

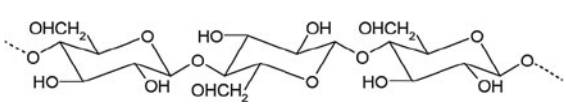

Fig. 2 The structure of cellulose

However, composites reinforced with natural fibers are not widely used in industrial applications mainly due to the following drawbacks: (1) cellulose fibers are polar and hydrophilic, so they are not compatible with non-polar and hydrophobic thermoplastics, which result in inefficient dispersion of the reinforcement and weak interaction between the matrix and reinforcement; (2) processing temperature limits the compounding of cellulose fibers with major engineering plastics such as polyethylene, polypropylene, polystyrene, and poly(vinyl chloride); (3) cellulose fiber-reinforced composites can be hygroscopic and swell causing a decrease in mechanical properties.

Overview of the theory of short fiber reinforced composites

Natural fibres are normally incorporated into short fibre-reinforced composites. Short fibre reinforced composites can be processed in a manner similar to the matrix, for instance injection moulding or extrusion for thermoplastics, which allows mass production of components. Cellulose fibres have been shown to exhibit better reinforcing potential than glass or carbon fibres in thermoset rubbery matrices (De and

Murty 1984). A possible reason is that flexible cellulose fibres are less damaged than brittle glass or carbon fibres during processing (Hamad 2002).

The stiffness of short fibre-reinforced composites can be predicted using the Halpin–Kardos model (Halpin and Kardos 1972). In this model, the properties of a heterogeneous solid reinforced with fibres of various orientations and asymmetrical geometries can be treated as a laminated solid. The solid is considered to be mathematically equivalent to a material composed of layers of oriented plies in which the ply properties are specified by the volumetric and geometric properties of the dispersion phases. When the fibres are randomly oriented, the laminate is known as "a quasi-isotropic laminate". The properties of this type of laminate can be approximated by using a model using four layers. Within each ply, the fibres are considered to be parallel to one another and the orientation of the plies is 0°, 45°, 90°, and −45° (see Fig. 3). This construct allows the elastic modulus of short-fibre reinforced composites to be predicted from three parameters: (1) the mechanical properties of fibres and matrix, (2) the volume fraction of the reinforcement, and (3) the aspect ratio of fibres. In this model, fibres are assumed to be embedded in the matrix to form a homogenous continuum, and separated so that there are no interactions between the reinforcement elements.

The mechanical properties of each ply can be derived from the Halpin–Tsai micromechanics equations (Tsai et al. 1968). The longitudinal Young's modulus of a ply, E_L, is given by:

$$E_L = E_m \frac{1 + 2\frac{L}{D}\eta_L \phi_f}{1 + \eta_L \phi_f} \tag{1}$$

where

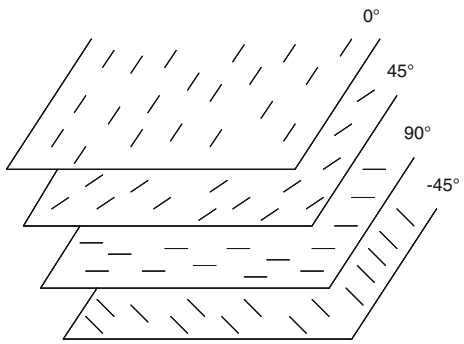

Fig. 3 The "quasi-isotropic" assumption in the Halpin–Kardos model (Halpin and Kardos 1972)

$$\eta_L = \frac{\frac{E_{lf}}{E_m} - 1}{\frac{E_{lf}}{E_m} + 2\frac{L}{D}} \tag{2}$$

here E is the Young's modulus, L/D is the aspect ratio of fibres, ϕ is the volume fraction of the specified phase, f and m in the subscripts refer to the fibre phase and matrix phase respectively, and E_{lf} is the Young's modulus of fibres in the longitudinal direction. In the transverse direction of the ply, the Young's modulus is:

$$E_T = E_m \frac{1 + 2\eta_T \phi_f}{1 - \eta_T \phi_f} \tag{3}$$

where

$$\eta_T = \frac{\frac{E_{tf}}{E_m} - 1}{\frac{E_{tf}}{E_m} + 2} \tag{4}$$

and E_{tf} is the transverse Young's modulus of fibres. Finally, the Young's modulus of the isotropic short fibre composite, E_c, is calculated as:

$$E_c = 4\frac{U_5}{U_1}(U_1 - U_5) \tag{5}$$

where

$$U_1 = \frac{1}{8}(3Q_{11} + 3Q_{22} + 2Q_{12} + 4Q_{66}) \tag{6}$$

$$U_5 = \frac{1}{8}(Q_{11} + Q_{22} - 2Q_{12} + 4Q_{66}) \tag{7}$$

$$Q_{11} = E_L/(1 - v_{12}v_{21}) \tag{8}$$

$$Q_{22} = E_T(1 - v_{12}v_{21}) \tag{9}$$

$$Q_{12} = v_{12}Q_{22} = v_{21}Q_{11} \tag{10}$$

$$Q_{66} = G_{12} \tag{11}$$

$$v_{12} = \phi_f v_f + \phi_m v_m = \frac{Q_{11}}{Q_{22}} v_{21} \tag{12}$$

$$G_{12} = G_m(1 + \eta\phi_f)/(1 - \eta\phi_f) \tag{13}$$

$$\eta = \frac{\frac{G_f}{G_m} - 1}{\frac{G_f}{G_m} + 1} \tag{14}$$

here v_f and v_m are Poisson's ratios, and G is the shear modulus.

As stated above, this model is based on the assumption that the short fibres have quasi-isotropic distribution in composites. In practice, however, processing may change fibre orientation, thereby

significantly affecting the mechanical properties of the final composite. Caution is therefore needed when applying this model. The randomness of the fibre orientation can be assessed by image analysis techniques to determine the fibre orientation distribution (FOD). Images are generally taken by cross-sectioning composite samples and using reflected-light microscopy (Whiteside et al. 2000) or scanning electron microscopy (Fung 2004). Computational image analysis will produce 2D analysis, while direct 3-D analysis can be obtained using confocal laser scanning microscopy (CLSM) (Clarke et al. 1995) and microwave techniques (Urabe and Yomoda 1991).

Cellulosic reinforcements

Wood is the major source of cellulosic fibres, especially for the pulp and paper industry, although a variety of other agri-fibres are available. Table 2 gives the production of some commercially important fibres that can be used in composites and their sources.

Wood fibres are defined by: the middle lamella, the primary wall, and the secondary wall (see Fig. 4). Cellulose microfibrils and hemicelluloses are present in all of the three regions. The third major component is pectin in primary walls and lignin in secondary walls. Wood is actually a composite of these materials, among which cellulose microfibrils impart wood strength (Panshin and de Zeeuw 1980).

Synthetic fibres have a specific range of properties, whereas the properties of natural fibres vary considerably with the source, location, age and processing of plants. With respect to the source, fibres can be obtained from animals or plant, and natural plant fibres can be grouped into: leaf, bast, seed, and fruit origin. Some examples of natural fibres and their physical properties are given in Table 3. For comparison, the properties of some typical synthetic fibres are listed as well.

One way to avoid the uncertainty of properties of natural cellulose fibers is to process them into a regenerated cellulose fibre suh as rayon, which was made possible over a century ago. The manufacture of rayon begins with cellulose, mainly from wood pulp, although any plant material containing cellulose with long molecular chains is suitable. After soaking in caustic soda solution, cellulose is reacted with carbon disulfide to produce a very viscous substance, which is then spun into rayon fibre. This process, however, has environmental challenges. Two decades ago, a new type of artificial cellulose fibre, lyocell or the brand name Tencel®, was first manufactured. Lyocell is produced by directly dissolving wood pulp in a non-toxic chemical solvent followed by spinning. The fibres are then washed and the solvent is recycled. Due to the closed-loop production process, it is environmentally benign. These types of regenerated cellulose fibers have

Table 2 Commercially important fibre production and sources (Suddell and Evans 2005)

Fibre	Species	World production (10^3 tonne)	Origin
Wood	>10,000 species	1,750,000	Stem
Bamboo	>1,250 species	10,000	Stem
Cotton lint	Gossypium sp	18,450	Fruit
Jute	Corchorus sp	2,300	Stem
Kenaf	Hibiscus cannadbinus	970	Stem
Flax	Linum usitatissimum	830	Stem
Sisal	Agave sisilana	378	Leaf
Hemp	Cannabis sativa	214	Stem
Coir	Cocos nucifera	100	Fruit
Ramie	Boehmeria nivea	100	Stem

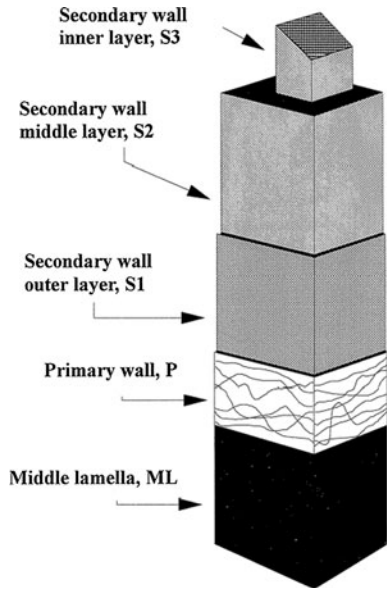

Fig. 4 A schematic of the detailed structure of cell walls. The secondary wall, which consists of 3 layers: *S1*, *S2*, and *S3* (Forgacs 1963)

Table 3 Physical properties of some natural plant fibres and their comparison to manmade fibres

Fibre	Density (g/cm^3)	Diameter (μm)	Tensile strength (MPa)	Young's modulus (GPa)	Elongation at break (%)	References
Bast						
Jute	1.3–1.45	25–200	393–773	13–26.5	1.16–2.0	Bledzki et al. (1996), Bisanda and Ansell (1992), Bledzki and Gassan (1999)
Flax	1.5	10–25	345–1,100	27.6	2.7–3.2	Grishanov et al. (2006), Bledzki et al. (1996), Bledzki and Gassan (1999)
Hemp	1.5	25–35	690	15–23	1.6	Eichhorn and Young (2004), Bledzki et al. (1996), Bledzki and Gassan (1999)
Ramie	1.5	10–25	400–938	61.4–128	1.2–3.8	Angelini et al. (2000), Bledzki et al. (1996), Zeronian (1991)
Leaf						
Sisal	1.45	50–200	350–640	9.4–22	3–7	Idicula et al. (2006), Bledzki et al. (1996), Bisanda and Ansell (1992)
PALF[a]	1.5	20–80	413–1,627	4.2–82.5	1.6–4	Idicula et al. (2006), Bisanda and Ansell (1992)
Seed						
Cotton	1.5–1.6	10–20	287–800	5.5–12.6	7–8	Zeronian (1991), Bledzki and Gassan (1999)
Fruit						
Coir	1.15	100–450	131–175	4–6	15–40	Bledzki et al. (1996), Bisanda and Ansell (1992)
Wood						
Wood kraft	0.6–1.1	20–40	980–1,770	10–80	1–4	Bailie (2005)
Synthetic						
E-glass	2.5	8–15	2,000–3,500	70	2.5	Bisanda and Ansell (1992), Saechtling (1987), Bledzki et al. (1996)
Aramid	1.4	15	3,000–3,150	63–67	3.3–3.7	Saechtling (1987), Bledzki et al. (1996)
Carbon	1.7	5–100	2,400–4,000	230–400	1.4–1.8	Bisanda and Ansell (1992), Saechtling (1987), Bledzki et al. (1996)

[a] *PALF* pineapple leaf fibre

properties that are tuneable over a wide range (Lenz et al. 1994; Fink et al. 2001; Kong and Eichhorn 2005).

Polymer composites

Cellulose fibre reinforced polymer composites

As the major source of cellulose fibers, wood fibers are widely used and studied in composites. Many polymers can be used as a matrix material, such as high density polyethylene (HDPE) (Hristov and Vlachopoulos 2007; Lei et al. 2007; Lu et al. 2005a, b), polypropylene (PP) (Nourbakhsh and Ashori 2008; Bledzki and Faruk 2006a; Karmarkar et al. 2007; Yuan et al. 2008), polyvinyl chloride (PVC) (Augier et al. 2007), low density polyethylene (LDPE) (Sretenovic et al. 2006), and ethylene vinyl acetate copolymer (EVA) (Dikobe and Luyt 2007). Biodegradable polymer matrices, including poly(lactic acid) (PLA) (Huda et al. 2006; Lee et al. 2008), polyhydroxybutyrate-co-valerate (PHBV) (Singh and Mohanty 2007), corn gluten meal (CGM) (Beg et al. 2005), and starch (Duanmu et al. 2007), have been attracting interest. Wood be used in composites in the form of fibre or particulate, for example as wood flour (Radovanovic et al. 2008) or saw-dust (Phiriyawirut et al. 2008).

Fiber reinforced polymer composites can be processed using conventional processing methods. A key point is the drying of the fibres before processing, since the water content in the fiber can result in weak adhesion between fiber and polymer, or even create voids in the composite when the water evaporates during processing. Bledzki and Faruk (2006b) studied microcellular PP composites reinforced with hardwood

fibers and compared the effect of processing methods—injection moulding, extrusion molding and compression molding—on the properties of the composites. In their experiments, wood fibers were dried at 80 °C in an air circulating oven for 24 h to reduce the moisture content to less than 1 %. They found that injection molding produced the best performance in terms of composite cell size,[1] shape and distribution, while the density was reduced by 30 % by inclusion of wood fibres. In another study, they compared the influence of processing temperature and reported that the resulting composites showed finer microcellular structure at the processing temperature of 160 °C, whereas the mechanical properties did not change over the temperature range 150–170 °C (Bledzki and Faruk 2006a).

Besides wood, polymer composites reinforced with other natural fibers, such as kenaf (Pan et al. 2008; Nishino et al. 2003; Zimmerman and Losure 1998; Chen and Porter 1994; Mehta et al. 2003), hemp (Thygesen et al. 2005; Keller 2003; Hokens et al. 2002), flax (Kaith et al. 2003; Bos et al. 2004; Manchado et al. 2003; Bos and Van den Oever 1999), jute (Sarkhel and Choudhury 2008; Alam et al. 2007; Khan et al. 2006; Doan et al. 2006; Sahoo et al. 2005; Datta et al. 2004) have been extensively studied. Natural fibres can also be combined with other reinforcements to form what is referred to as hybrid composites to further improve the overall properties. In a series of studies, Maldas and Kokta (1990, 1991a, b, c, 1992) investigated the properties of composites filled with wood (fibre or sawdust) and glass fibres/mica. They found that the surface treatments of the fillers were critical for the performance of the composites. Thwe and Liao (2000, 2003) prepared PP based composites reinforced with bamboo and glass fibres and studied the mechanical properties and aging effects of these composites. They concluded that the addition of glass fibres can improve composite properties significantly. The composite with 10 % bamboo fibers and 10 % glass fibers had 21 and 31 % increase in tensile strength and tensile modulus respectively, compared with 20 % increas in strength when using bamboo fibers only. Mixtures of natural fibers were also employed. For example, Tajvidi et al. (Tajvidi 2005; Mirbagheri et al. 2007) prepared PP composites filled with wood flour (WF) and kenaf fibres (KF). They found that KF and WF composites had the highest and lowest strengths, respectively, while the strength of the hybrid composites was in between and determined by the ratio of WF to KF.

Although most of the cellulosic fibres applied in composites are from natural sources, regenerated cellulose fibres, namely rayon or lyocell, have been studied as well. Adusumalli et al. (2006) characterized a large number of regenerated cellulose fibres using single-fibre tensile tests and compared the results with those of glass fibres and natural flax fibres. The results, which are listed in Table 4, demonstrated that regenerated cellulose fibre composites had less strength and modulus compared to glass fibre reinforced composites, but performed well in terms of work to fracture. Flax fibre reinforcement outperforms regenerated cellulose in strength and stiffness, but not in work to fracture (energy absorption). Since regenerated cellulose fibres have a chemical composition similar to natural fibres, they also have problems with compatibility with thermoplastics, often coupling agents become necessary (Trejo-O'Reilly et al. 2000). It should be noted that a new generation of high-modulus lyocell fibres have been manufactured for demanding structural applications, and as such, can potentially compete with glass reinforcement.

A major potential application of cellulosic fibre reinforced composites is the automotive industry because of the need for light-weight, durable, inexpensive and potentially recyclable parts (Suddell and Evans 2003). In comparison to conventional glass and mineral filler, natural fibres are strong, lightweight, low-cost, environmentally friendly, and more importantly, they can provide comparable stiffness enhancement and better sound damping. The application of these composites in automotive components is forecast to increase by 54 % per year, mostly in interior parts (Report 2002). For further details on the application of bio-fibre composites in automobiles, there is a review article on this topic (Bledzki et al. 2006). With rapid fluctuation in petroleum prices and concerns about global environmental changes, it can be foreseen that the application for natural fibre based composites will likely quickly expand.

Surface treatment of cellulosic reinforcements

A very common problem in cellulose fibre based composites is the compatibility of fibres and polymers, because fibres are highly polar and hydrophilic

[1] Cell here refers to a physical unit comprising a single fibre-matrix and their interactions.

Table 4 Average tensile properties of regenerated cellulose in comparison to glass and natural fibres

E—modulus of elasticity, σ_f—tensile strength at break, ε_f—elongation at break, $W_{\varepsilon f}$—work to fracture, adopted from (Adusumalli et al. 2006)

	E (GPa)	σ_f (MPa)	ε_f (%)	$W_{\varepsilon f}$ ($J*10^{-3}mm^{-3}$)
Viscose	10.8 ± 2.5	340 ± 73	15.4 ± 2.2	32.7
Modal	13.2 ± 2.2	437 ± 69	10.4 ± 1.8	37.2
Lyocell	23.4 ± 3.9	556 ± 78	8.7 ± 1.6	34.5
Rayon tirecord	22.2 ± 1.0	778 ± 62	10.7 ± 1.4	40.8
Flax	40.0 ± 19.2	904 ± 326	1.4 ± 0.2	6.7
Glass	70.0 ± 9.3	3,000 ± 356	4.3	54.3

whereas most polymers are non-polar and hydrophobic. To solve this problem, fibre surfaces can be treated using physical, physico-chemical or chemical methods depending on the polymer matrices to be used (Belgacem and Gandini 2005b). The cellulose hydroxyl groups can be used to prepare a variety of cellulose derivatives. Ideally the modifications need to be limited to the surface hydroxyl groups to preserve the integrity of the fibres and thus their mechanical strength.

Physical methods Physical methods, such as stretching (Zeronian et al. 1990), calandering (Semsarzadeh 1986), and thermotreatment (Ray et al. 1976) alter the structural and surface properties of fibres to enhance the mechanical bonding to polymer matrices without changing the chemical composition of fibres. In a study conducted by Boufi and Gandini (2001), a novel approach was developed by enveloping cellulose fibres with a thin sleeve of polymer, without any chemical interaction with the fibre surface. This was realized by adsorbing cationic surfactants onto fibres suspended in water to form an admicellar (adsorbed micelle) structure followed by polymerization of water-insoluble monomers, e.g. styrene and acrylates, in the hydrophobic double layers. The free radical polymerization generated a thin polymer coating around the fibres, which could be detected with electron microscopy and FT-IR. These thin coatings change cellulose fibre properties significantly. For example, the presence of a polystyrene coating increased the contact angle from 30° to 90° and changed the surface character from acidic to amphoteric.

Physico-chemical methods Physico-chemical treatments can purify, oxidize and/or activate the fibre surfaces. These include corona treatment, plasma treatment, laser treatment, vacuum-ultraviolet treatment, and γ-ray treatment. Below are some examples.

Corona treatment This technique can improve the bonding characteristics of materials by raising the surface energy slightly. Uehara and Sakata (1990) treated beech wood using a corona in a stream of air or nitrogen at 20 °C and 72 % relative humidity. The FT-IR spectra showed a band at 1,715 cm^{-1} indicating that aldehyde groups were introduced onto fibres. It was also found that some basic groups were formed in the case of long treatment times under nitrogen, while chain scission would occur if the treatment was conducted in air. Sawatari et al. (Nishiyama et al. 1993; Sawatari and Nakamura 1993) studied corona treatment on Whatman #1 filter papers, regenerated cellulose films, hand sheets from thermo-mechanical pulp (TMP) and hand sheets from softwood bleached kraft pulp (SBKP). The discharge conditions were 13 kV, 4 W and 50 Hz in a stream of oxygen at atmospheric pressure and room temperature for up to 1 h. The X-ray photoelectron spectroscopy (XPS) analysis results revealed that this treatment generated carbonyl and carboxyl groups on the substrate surfaces, which could be used for subsequent grafting reactions. Bataille et al. (1994) activated the surface of Whatman #42 filter paper by corona discharge using currents of 7–20 mA and an exposure time of up to 10 min, and then immersed the treated paper in a methanol-styrene solution. They found that polystyrene can be grafted onto cellulose surface in this way at a coverage of 2–7 g polymer per square meter of paper. The contact angle of a drop of water deposited on the treated filter paper increased from practically 0° to about 100° at the coverage of 3 g/m^2 and the penetration time of water into the filter paper increased from a few seconds for untreated samples to 120 s when the polymer coverage was 1 g/m^2. Gel

permeation chromatography (GPC) results demonstrated that the molecular weight distribution of the grafted polymer was bimodal, with molecular weights of 700 and 75 kDa, respectively.

Plasma treatment In the last few decades, cold-plasma chemistry has been used to modify the surfaces of various materials, especially polymers, by using specific molecules in the gas phase. The application of this technique to cellulose started with the improvement of cotton wettability (Benerito et al. 1981) and the adhesion between paper laminates and polyolefins (Westerlind et al. 1987). Carlsson and Ström (1991) investigated hydrogen and oxygen plasma treatments to two cellulose materials, a filter paper of pure cellulose and a greaseproof paper with a fairly high surface content of wood resin. They concluded that hydrogen plasma reduced the hydroxyl groups on the cellulose and low molecular weight materials were formed. The water wettability of pure cellulose was reduced, but for paper with high resin content on the surface the wettability was improved. The wettability of greaseproof paper was improved after oxygen plasma treatment by means of oxidizing and reducing the surface. Plasma can also be used to generate free radicals on the cellulose surface, which can be used to initiate grafted polymers. By using electron spin resonance (ESR), Sabharwal et al. (1993) investigated the formation of free radicals in jute treated with argon plasma. They found that lignin was the primary site of free radical formation and 2–3 min of treatment time was sufficient to maximize free radical production and avoid quenching reactions. The generated free radicals diminished drastically in less than a minute under atmospheric conditions, which suggests that the second stage grafting polymerization initiated by the free radicals should be carried out under inert gas or vacuum. Felix et al. (1994) modified cellulose fibres with plasma treatment and found that although the surface treatment was incomplete, it was effective to controllably alter the acid/base interaction balance of the fibre surface. The modified fibres were then used in composites with polystyrene, chlorinated polyethylene, and polypropylene as basic, acidic, and neutral matrices, respectively. Favourable acid/base interactions led to enhanced mechanical properties and increased glass transition temperatures of composites. As expected, it was proved that the acid/base consideration was irrelevant for the PP composite.

Laser treatment The major studies using this technique focused on the molecular weight change of the treated materials, rather than the surface properties. Kolar et al. (2000) evaluated the applicability of excimer laser at 308 nm and Nd:YAG laser at 532 nm with fluences[2] below 0.86 J/cm^2 for cleaning of cellulose and paper materials. They found that the degree of polymerization (DP) of the cellulose materials remained constant when the excimer wavelength was 532 nm, whereas the laser with 308 nm wavelength resulted in detrimental effects on DP and the brightness of the filter paper. Botaro et al. (2001) studied the effect of Nd:YAG pulsed laser (wavelength = 1,064 nm) on Whatman #5 filter paper, microcrystalline cellulose, and organosolv lignin. They found that lignin suffered great weight loss and structure change, whereas the treatment only had negligible effect on cellulose. Mizoguchi et al. (2001) studied the effect of different excimer laser beams (ArF, KrF and XeCl with wavelengths of 193, 248 and 308 nm, respectively) on the treatment of regenerated cellulose surface. The results demonstrated that the surface structure changed only when ArF laser was applied and the extent of the change was strongly related to the fluence and the number of pulses. After treatment, the tensile strength of fibres decreased while the moisture content increased slightly.

Vacuum-ultraviolet (VUV) treatment This method is rarely used for cellulose surface modification. Kato et al. (1999) used this approach to oxidize cellulose fibres to introduce carbonyl and carboxylic acid groups onto the fibre surface, and compared the efficiency of this method with conventional techniques, such as oxidation with chromic acid, nitric acid, ozone and hydrogen peroxide methods. They concluded that the efficiency of the VUV method was comparable to chromic acid and nitric acid and better than ozone and hydrogen peroxide. Compared to the wet process of using acids, VUV irradiation is dry and clean without changing the bulk mechanical properties of fibres.

γ-Ray treatment *γ-Ray* has high energy, therefore it causes degradation of cellulose when treating fibres with it. In a series of studies using γ-irradiation to treat

[2] Fluence is defined as the number of particles that intersect a unit area. The term is used in particular to describe the strength of a radiation field.

cotton fibres (Takacs et al. 1999), it was reported that the DP of cellulose decreased from 1,200 to 330 at an irradiation dose of 15 kGy. However, the degradation could be limited by pretreating the cellulose fibre with a base, which may have allowed chain coupling through radical recombination, i.e. crosslinking. Because of the high energy of this treatment method, it is not typically suitable, or cost effective, for surface modification of cellulose fibres.

Chemical methods The chemical modification methods are the most widely studied and used approaches to modify cellulose surfaces. They can be classified into two main categories: surface compatibilization and co-polymerization. In the first category, the main idea is to use a simple coupling reaction between the surface hydroxyl groups on cellulose fibres and molecular or macromolecular agents bearing one or more –OH reactive functional groups. These agents can have a single reactive moiety or many along a polymer chain. Figure 5 shows some examples of these types of agents. Co-polymerization is the second category and it includes four strategies: (1) Grafting with polymerizable molecules. This approach uses small molecules bearing two functional groups, one of which can react with the –OH on cellulose, and the other of which can covalently bond to the matrix polymer. This method can be applied in both polyaddition polymerization and polycondensation polymerization. (2) The use of planar stiff molecules. This method uses molecules with two identical reactive moieties, one of which can react with the cellulose –OH group, but the other one cannot because of the stiff and planar structure of the molecule and the reaction conditions. Thus, it can subsequently react with the matrix polymers. This approach is suitable for matrices formed by polycondensation reactions. (3) Direct activation of the cellulose surface to generate an active centre, for example a free radical, to initiate a suitable monomer. (4) Reaction with organometallics. This method uses a similar idea to that in (1), but uses organometallics instead to treat fibre surfaces.

Compared to chemical methods, the physical and physico-chemical methods do not need complicated chemical reactions and the purification process to remove unreacted substances, thus they are cleaner and simpler than the chemical methods. Moreover, the modification of cellulose fibres via physical and physico-chemical methods can be limited to the cellulose surfaces to avoid any damage to the fibre interior, which can diminish the mechanical properties of fibres. However, the physical methods only offer a limited improvement of the compatibility between fibres and polymer matrices as they cannot essentially change the surface properties of the fibres. Physico-chemical methods usually need special instruments, which increase the cost and make the approach unsuitable for large-scale mass production. Chemical

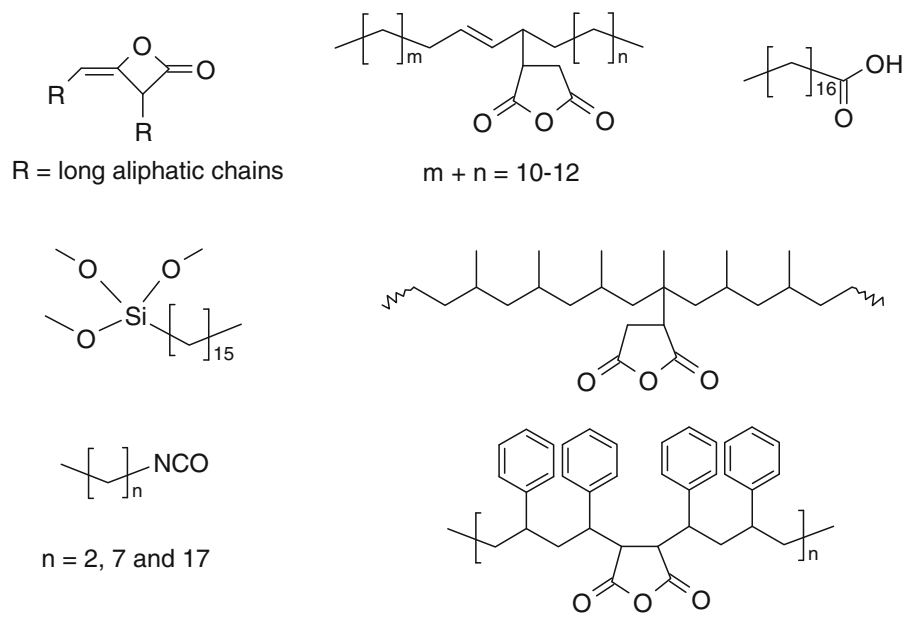

Fig. 5 Examples of the agents that react with –OH on cellulose (Quillin et al. 1992, 1993, 1994; Castellano et al. 2004; Joly et al. 1996)

methods are more specific and numerous. The selection of modification methods is determined largely by cost, the type of fibres and matrices, and the composite processing conditions.

A variety of techniques can be applied to characterize the modified fibre surface including Fourier transform infrared spectroscopy (FT-IR), X-ray photoelectron spectroscopy (XPS), elemental analysis, inverse gas chromatography (IGC), scanning electron microscopy (SEM), contact angle measurements, nuclear magnetic resonance (NMR), confocal laser scanning microscopy (CLSM), and atomic force microscopy (AFM) (Belgacem and Gandini 2005a, b; Mohanty et al. 2001).

Cellulosic micro and nano reinforcement

It is well known that pure cellulose microfibrils have high strength due to their highly crystalline structure and the existence of inter- and intra-molecular hydrogen bonds. Natural cellulosic fibres, however, have much lower strength than the theoretical value of cellulose because of the existence of amorphous cellulose regions and other components such as hemicellulose. In order to fully utilize the features of cellulose, effort has been made to obtain cellulose microfibrils with unique properties, especially high strength, by controlled disintegration of natural fibres or growing cellulose from bacterial sources. The obtained cellulosic structures are usually at the micron or nanometer scale, and can demonstrate special properties when used as reinforcement in polymer composites. In this section, preparation methods and properties of microfibrillated cellulose, microcrystalline cellulose, bacterial cellulose, and nanocrystalline cellulose are discussed in detail.

Microfibrillated cellulose

Microfibrillated cellulose (MFC) was first produced three decades ago by Turbak et al. (1983). In their experiments, wood pulp sheets were precut to reduce fibre length to 0.6–0.7 mm, and then passed through a small commercial homogenizer repeatedly using a pressure of 55 MPa. During homogenization, the product temperature was controlled in the range 70–80 °C, and the cellulose microfibrils, which are ordered bundles in the fibre walls, were separated and unravelled by the applied high mechanical forces to produce a mesh of fibrils and microfibrils with diameters of about 25–100 nm. A SEM micrograph of MFC produced by this method (20 passes of homogenization in a 1 % water dispersion) is shown in Fig. 6. The influence of the homogenization process on the degree of polymerization (DP) was small. According to an example given by Turbak et al. (1983), the DP of the original pulp only decreased from 2,501 to 2,202 after homogenization. One of the major drawbacks of this method is its high energy consumption. Spence et al. (2011a) studied energy consumption of MFC production using different methods, and compared their effects on the physical properties of MFC. The authors investigated three approaches to prepare MFC, including homogenization, microfluidization, and micro-grinding. They found that there were large differences in the specific energy consumption on solid basis per pass: 3,940 kJ/kg (1,095 kWh/ton) and 620 kJ/kg (170 kWh/ton) for homogenizer and micro-grinder, respectively. The microfluidizer energy measurements were 200, 390, and 630 kJ/kg (56, 110, 175 kWh/ton) per pass for processing pressures of 69 MPa (10 kpsi), 138 MPa (20 kpsi), and 207 MPa (30 kpsi), respectively. Based on these and the energy consumed in a pre-treatment process in a Valley beater, the total energy consumption to produce MFC from bleached hardwood (BHW) and unbleached hardwood (UBHW) were calculated and part of the results are summarized in Table 5. Compared to homogenization, the energy consumption is much lower in microfluidization, and especially

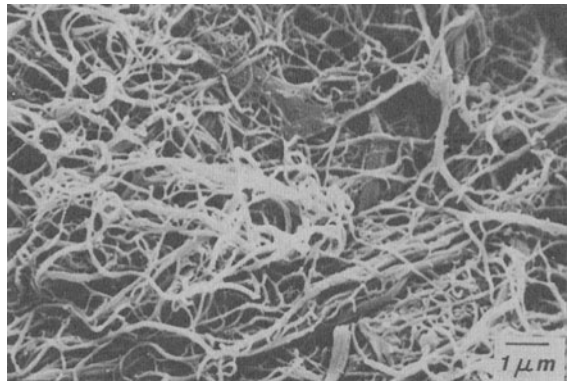

Fig. 6 SEM micrograph of microfibrillated cellulose (MFC) (Turbak et al. 1983)

in micro-grinding, where the pre-treatment step can be reduced or eliminated. The authors also concluded that the MFC produced by microfluidization and micro-grinding has better mechanical properties than that from homogenization in terms of tensile index and toughness. However, homogenization is superior to the other two methods insofar as producing MFC with larger specific surface area.

To reduce the high energy cost, pre-treatments on fibres prior to mechanical processing have been studied, including acid hydrolysis (Boldizar et al. 1987), TEMPO-mediated oxidation (Saito et al. 2006), and enzyme treatment (Henriksson et al. 2007). By combining pre-treatments with mechanical processing, it is possible to reduce the energy consumption to the level of 1,000 kWh/ton (Siró and Plackett 2010). For acid hydrolysis treatment, pulps were hydrolyzed in a variety of conditions: the acids employed include HCl and H_2SO_4; and acid concentrations varied from 1 to 2.5 M; the reaction temperature and time were in the range of 70–100 °C and 1–4 h, respectively. As a consequence, the DP of the pulp dropped from 1,390 to 267–343 (Boldizar et al. 1987). Thereafter, the hydrolyzed pulps were treated by homogenization. Saito et al. (2006) pretreated pulps with TEMPO (2,2,6,6-tetramethyl-1-piperidinyloxy), which can catalyze the oxidation of hydroxyl groups on cellulose and introduce negative charge. In their experiments, the oxidation was carried out on never-dried cellulose (bleached sulfite wood pulp, cotton, tunicin, and bacterial cellulose) at room temperature and basic condition. After homogenization, although the fibrils were well individualized, no isolated cellulose microfibrils could be observed under TEM, even after extensive dilution. The widths of the obtained microfibrils were from a few nanometers to several tens of nanometers depending on the sources of fibres. There was no DP data provided in this paper. However, Srithep et al. (2012) also employed TEMPO-mediated oxidation as a pre-treatment to pulps in a similar manner to Saito's. Instead of homogenization, they refined the fibres using a disc refiner with a gap of 200 μm following an oxidization step, and subsequently removed the coarse fibres by centrifugation. Finally, the fibre suspension was passed once through a microfluidizer with 200 and 87 μm chambers in series to obtain MFC. The resulting MFC is an interconnected web with fibrils having a diameter in the range of 10–50 nm. Moreover, Henriksson et al. (2007) pretreated pulp using enzymes, where the wood pulp was first mechanically beaten 1,000 revolutions in a PFI-mill with a dry pulp content of 13.3 %. As such, the fibres became more swollen by water to make the cellulose more accessible to the enzymes. The fibres were then treated using the enzyme Novozym 476, an endoglucanase, and were subsequently beaten again with 4,000 revolutions in a PFI-mill. After these pre-treatments, the fibre suspension was passed 20 times through a high-pressure slit homogenizer. The microfibrils obtained in their work were about 15–30 nm wide and several micrometers long. The DP of fibres, however, decreased greatly from 1,280 to 340–740 (depending on treatment conditions) for the case of a softwood dissolving pulp. Instead of the homogenization method, a group at the University of Toronto developed a cryocrushing approach to individualize the microfibrils from cell walls (Chakraborty et al. 2005). In their approach, pulps were first refined with a PFI-mill for up to 125,000 revolutions to break down the surface structure of fibres. The refined fibres were subsequently crushed in liquid nitrogen with a cast iron mortar and

Table 5 Parameters and energy used to produce MFC from wood pulp fibres by homogenization, micro-grinding, and microfluidization (Spence et al. 2011a)

Processing method	Valley beater pretreatment	Pressure or speed	Number of passes (chamber[a])	Total energy consumption [kJ/kg(kWh/ton)]
Valley beater pretreatment				7,230 (2,008)
Homogenizer	Yes	55 MPa	20	78,800 (21,889)
Micro-grinder	No	1,500 rpm	9	5,580 (1,150)
Micro-grinder	Yes	1,500 rpm	9	12,810 (3,558)
Microfluidizer	Yes	69 MPa	20 (H210Z)	11,230 (3,119)
Microfluidizer	Yes	69 MPa	5 (G10Z)	8,230 (2,286)

[a] Chambers on microfluidizer: H210Z = Z configuration, 200 μm orifice; G10Z = Z configuration, 100 μm orifice

pestle. The majority of the microfibrils produced using this method had diameters in the range 0.1–1 μm, which is bigger than those described above. They then modified this approach by adding a series of chemical treatments with acid and base to fibres before the cryocrushing step (Bhatnagar and Sain 2005). The diameters of microfibrils obtained in this way were in the range of 10–60 nm. Figure 7 is a TEM image of MFC made via cryocrushing. By comparing Figs. 6 and 7, there is no distinguishable difference between the MFCs made by these two types of methods in terms of the net-like structure.

Besides direct mechanical forces, other methods were also explored to free cellulose fibrils. Frone et al. (2011) reported preparation of MFC from microcrystalline cellulose (MCC) using an ultrasonicator. In their method, low concentration MCC water suspensions (0.2 wt%) were sonicated for 10 or 20 min at 200 or 400 W power first at controlled temperature (below 50 °C). After settling for 2 h, the supernatants, i.e. the MFC suspensions, were decanted and collected as the MFC products. The yields of MFC from this method are low, which is only 7.8–27.6 %. On top of that, the actual energy consumption per kilogram of MFC is even several times higher than those prepared by homogenization. Therefore, this method is not suitable for practical application.

MFC is also referred as nanofibrillated cellulose (NFC) when sufficient energy is applied so that the diameter of fibrils is completely broken down to nanometer scale, normally below 100 nm. Essentially, both MFC and NFC are webs of cellulose microfibrils obtained by exerting strong mechanical forces on cellulose fibres to break up the fibre wall structure. All of the preparation methods require energy intensive physical techniques—namely, refining followed by homogenization/microfluidization/micro-grinding and/or cryocrushing. Although, some modification methods were investigated to reduce energy consumption by adding pretreatment procedures before applying physical forces, these extra steps (chemical or enzymatic) prolong the preparation time and increase the cost. The diameters of individual microfibrils obtained through any of these approaches are usually smaller than 100 nm, however, they cannot be separated to obtain discrete units. Rather, the microfibrils in MFC are always in a net-like formation. No literature has ever reported achieving discrete isolated cellulosic nanostructures of distinct physico-chemical properties through primarily physical approaches.

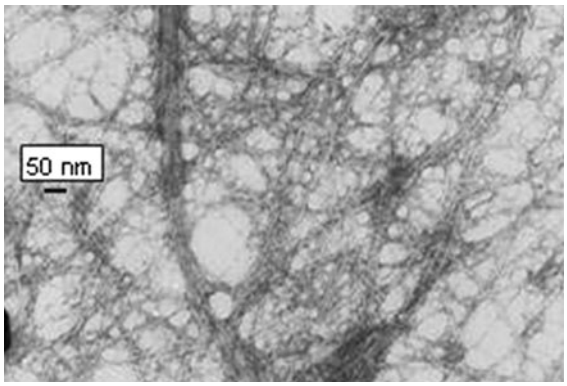

Fig. 7 A TEM micrograph of negatively stained MFC made from rutabaga by cryocrushing approach (Bhatnagar and Sain 2005)

MFC, albeit fibril-like in appearance, is merely fragmented cell wall material rather than pure cellulose fibrils. The strength of sheets made from MFC, but not of a single microfibril in the MFC mesh, has been studied. Taniguchi and Okamura (1998) prepared MFC, from wood pulp, using a small commercial grinder with a specially designed disk (super-grinding), and made films from the MFC on a plastic plate with a film applicator. The tensile strengths of the obtained films were characterized. They did not give a value for the tensile strength, but only showed a comparison index based on a commercial print grade paper. According to their results, the strength of the MFC film was about 2.4 times that of print grade paper. Henriksson et al. (2008) prepared a series of MFCs with different DPs ranging from 410 to 1,100 by changing the pretreatment conditions. Sheets were made using their lab-prepared MFC by vacuum filtration of the MFC suspensions on filter paper or membrane, a procedure similar to that in making conventional handsheets. The authors tested the tensile properties of the sheets and the results are summarized in Table 6. It can be found that the tensile strength and the work to fracture increased with the DP of MFC, but the modulus was insensitive to the DP. It is well-known that paper strength is dependent on both the fibre strength and the fibre–fibre bonding strength (Page 1969), which can be extended to MFC sheets—as they are also fibre networks similar to regular paper sheets. The higher strength of MFC sheets can be explained by the fine structure of MFC, because on the one hand, the microfibrils in MFC can form very

Table 6 Tensile properties of MFC films prepared from MFC with different DP (Henriksson et al. 2008)

Material	Modulus (GPa)	Tensile strength (MPa)	Strain-to-failure (%)	Work to fracture (MJ/m^3)
DP-410	13.7 ± 0.3	129 ± 8.7	3.3 ± 0.4	3.0 ± 0.5
DP-580	10.7 ± 1.2	159 ± 16.4	6.4 ± 1.7	7.1 ± 2.5
DP-820	10.4 ± 0.5	181 ± 12.7	7.4 ± 1.5	9.1 ± 2.3
DP-1100	13.2 ± 0.6	214 ± 6.8	10.1 ± 1.4	15.1 ± 1.9

compact architecture, which allows more hydrogen bonds to form among them, and, on the other hand, there exist more interfibrillar entanglements. The measurement of the strength of a single fibre using conventional method is difficult, as it requires special instruments and the results are easily influenced by the testing conditions.[3] Tanpichai et al. (2012a) evaluated the Young's modulus of single MFC fibrils indirectly using their well-established Raman spectroscopy techniques and estimated the effective modulus to be 29–36 GPa. More recently, Saito et al. (2013) measured the strength of single cellulosic nanofibrils using sonication-induced fragmentation—a high volume statistical approach constructed on the basis of a model for the fragmentation of filamentous nanostructures under the action of hydrodynamic stresses imparted through sonication-induced cavitation. They reported values of 1.6–3 GPa for nanofbrils from wood and 3–6 GPa for the fibrils from tunicate.

It is also of interest to apply MFC films as food packaging materials due to its low oxygen transmission rates, renewability, and safety to food. The water vapor barrier properties of MFC, however, are not satisfying because of its hydrophilic nature. Rodionova et al. (2011) reported a possible approach to reduce water vapor transmission rate (WVTR) of MFC by chemically modifying the MFC surface via heterogeneous acetylation. The reactions between MFC and acetic anhydride were carried out in toluene. After comparing the products from different reaction times, it was found that the modified MFC films with 0.5 and 1 h reaction time could reduce WVTR to 167 g/m^{2}day compared to 234 g/m^{2}day of unmodified MFC. However, WVTR increased to 256 and 264 g/m^{2}day when the reaction time was prolonged to 3 and 4 h, respectively. The authors ascribed the initial drop of WVTR to the decreased hydrophilicity of MFC. With the increase in reaction time, more hydrogen groups were acetylated resulting in less hydrogen bonds between the microfibrils, thus a more open network structure of MFC. Spence et al. (2011b) improved WVTR of MFC by adding fillers in MFC films or adding coatings on the surface of MFC films. The fillers were introduced in MFC by mixing them in MFC suspension before film-casting. The authors compared 0.1–2.5 μm calcium carbonate and 0.5–10 μm kaolin clay and found that kaolin clay is more effective to reduce WVTR. For example, at 7.5 % addition, kaolin clay and calcium carbonate can reduce WVTR 51.6 and 21.4 %, respectively. This was explained by the lower solubility of water vapour through filler materials, which was indicated by the increased tortuosity and path length through MFC films. On the other hand, the authors also adding coatings on the surface of MFC films by dipping the films in coating solutions. It was found that at coating weights of approximately 1 g/m^2 of beeswax, 2.5 g/m^2 of paraffin, and 5 g/m^2 of cooked starch, the WVTR of MFC films was lowered to about half that of LDPE (Fig. 8). Further increase in the coat weight (of paraffin and cooked starch) did not significantly reduce WVTR, whereas beeswax could further decrease WVTR at higher coat weights. This was ascribed to the ability of beeswax to penetrate into MFC films, whereas the coating of paraffin and cooked starch mainly stay on the surface of films. The authors finally concluded that coatings reduce WVTR of MFC films by closing the surface pores and filling the pore network, thereby resulting in a multilayer structure.

MFC has also been used as reinforcement in polymer composites. Nakagaito and Yano (2004, 2008a, b) investigated the mechanical properties of phenol–formaldehyde (PF) resin based composites reinforced with MFC and compared the results with

[3] A conventional method to examine pulp fibre strength is to measure the zero-span strength of paper sheets. In order to compare the strength of individual MFC microfibrils with pulp fibres, the zero-span strength, or some similar concept, of MFC sheets and paper sheets is needed.

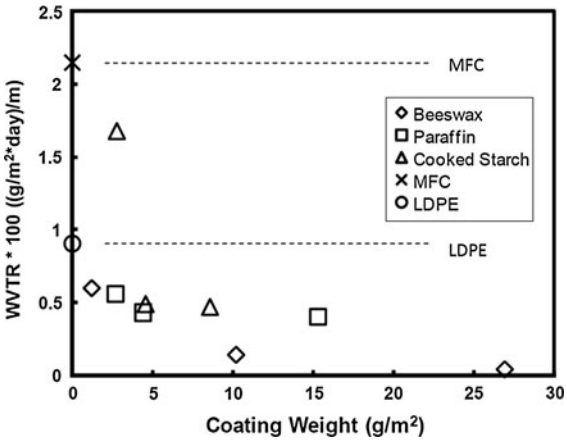

Fig. 8 Water vapor transmission rate (WVTR) of microfibrillated cellulose (MFC) films coated with beeswax, paraffin, and cooked starch at varying coating weights (Spence et al. 2011b)

those of composites reinforced with ordinary wood fibres. The composites were prepared by soaking dried (air dried or freeze dried) MFC or pulp sheets in PF resin diluted with methanol to a variety of concentrations. After drying, the composite sheets were hot pressed. For the composites made from air-dried sheets, the results revealed that the MFC and pulp based composites had similar Young's modulus when compressed at 100 MPa. The MFC-based composites had about 50 % higher bending strength than the pulp-based ones within the tested range of PF resin content. They also impregnated freeze dried MFC and pulp sheets with PF resins to increase the resin content in the composites. The strength test results demonstrated that there was no obvious difference between the MFC and pulp based composites when compared at a similar fibre content. Pre-treatments to MFC sheets with NaOH aqueous solution before impregnation were also investigated. The testing results exhibited that the alkali-treatment had no significant effect on the strength and modulus of MFC composites, but only improved the work-to-fracture. For example, with resin content around 20 wt%, the work-to-fracture was two times higher than those of untreated MFC composites. This improvement was attributed to the ductility of the fibrils caused by transformations in the cellulose amorphous regions (Nakagaito and Yano 2008b).

MFC and polylactic acid (PLA) composites have also been studied. Iwatake et al. (2008) prepared MFC/PLA composites by compounding them in a twin rotary roller mixer at 140 °C. The compound was then crushed and hot pressed for strength testing. The resulting composites had improvements of 40 and 25 % in Young's modulus and tensile strength, respectively, without a reduction in yield strain at 10 wt% fibre content. Chakraborty et al. (2005) also tried to mix their cryocrushed MFC with PLA by compounding PLA and MFC[4] water suspension in a twin screw Brabender mixer at 190 °C, followed by hot pressing. They did not report any mechanical properties of the resulting composite, but only observed the distribution of MFC fibrils in PLA under CLSM. They concluded that MFC was well dispersed in PLA through such a processing procedure. 71 % of the MFC applied in their experiment had diameters in the range of 0.1–1 μm.

Mathew et al. (2006) compounded MFC with PLA using a twin screw extruder and studied the mechanical properties of the resulting composite (Table 7). The direct addition of MFC had no effect on the composite strength. Since MFC might not be well dispersed in PLA under these processing conditions, the authors used polyethylene glycol (PEG) to improve dispersion. The results were still unsuccessful. Instead of physical mixing by co-extrusion, Tanpichai et al. (2012b) prepared MFC/PLA laminated composites via compression moulding. They first cast MFC films ~80 μm thick in water, and placed them between two PLA films (thickness ~110 μm) compressed in a hot metal mould, followed by compression at 12 MPa and 180 °C. The thickness of the final composite was ~200 μm and the MFC content in the composite was 20.5 ± 1.5 wt%. Compared to neat PLA films, the improvement in mechanical properties was not significant, which was not surprising since the MFC network used in their work did not possess high strength (according to their own data). However, the main finding of their work was the observation of stress transfer between the MFC network and PLA. This was supported by two characterization results: the penetration of PLA into the MFC network observed under SEM, and the shift of a 1,095 cm^{-1} Raman-sensitive band (characteristic of cellulose) towards a lower wavenumber. Boissard et al. (2012) prepared MFC/PLA cellular composites using a wet compounding process followed by

[4] Stained with calcofluor dye for observation using a confocal laser scanning microscope.

Table 7 Mechanical properties of PLA and its composites reinforced by MFC (Mathew et al. 2006)

	Tensile strength (MPa)	E. Modulus (GPa)	Elongation (%)	Toughness (kJ/m^2)
PLA	58 ± 6	2.0 ± 0.2	4.2 ± 0.6	35 ± 8
PLA + 5 % MFC[a]	58 ± 5	2.6 ± 0.1	2.8 ± 0.5	24 ± 8
PLA + 5 %PEG[b]	51 ± 3	2.1 ± 0.6	[c]	[c]
PLA + 5 %PEG + 5 % MFC	59 ± 2	2.3 ± 0.1	3.3 ± 0.2	27 ± 2

[a] The percentages were measured in weight

[b] *PEG* polyethylene glycol, was used as a processing aid to decrease the viscosity of the system, thus helping the dispersion of reinforcement

[c] The toughness could not be calculated because the samples had very high elongation without breaking

supercritical carbon dioxide ($ScCO_2$) foaming. In their work, MFC and powder form PLA were mixed evenly in water suspension and MFC/PLA mixture was obtained after dewatering. Through such a process, MFC forms a network in the mixture. After drying, the mixture was compression-moulded to form a plaque, which was used for foaming in $ScCO_2$. However, the hydrogen bonds in the MFC network seriously impeded expansion of PLA during the foaming process. To overcome this, the MFC/PLA plaques were processed by extrusion before foaming to weaken the MFC network. The authors proposed that the hydrophilic MFC accelerated hygrothermal degradation of PLA during processing, thus resulting in poorer foamability and mechanical properties. It was further noted that the addition of a chain extender during extrusion seemed to be effective in offsetting the effect of molecular degradation. After the extrusion and foaming processes, it is highly doubtful that any MFC network remains structurally intact in the final MFC/PLA foam to contribute to improving the final properties.

In another example, Henriksson and Berglund (2007) used another way to prepare MFC composites. They filtered MFC water suspensions through a filter paper to make MFC films. After drying, the MFC films were soaked in melamine formaldehyde (MF) solution with different concentrations to vary the MF content in the MFC films. Then, the MF was cured by hot pressing to obtain composites. The mechanical properties of these composite films are presented in Table 8. In such composites, however, MFC was the major composition, and the best performing sample contained 95 wt% MFC. In the case of 95 wt% MFC, the tensile strength and modulus were increased by 40 and 15 % relative to the sample containing 100 wt% MFC. However, there was a significant drop in stretch (>−40 %) and toughness.

Another investigated polymer matrix is polyvinyl alcohol (PVA). Chakraborty et al. (2006) prepared MFC/PVA composites by film casting and examined their tensile properties. The results were compared with those of composites made by the same method but reinforced with bleached kraft pulp (BKP) and microcrystalline cellulose (MCC). It was found that MFC had the best reinforcing effect among the three reinforcements when the mass fraction was 5 % in the composites. However, increasing MFC loading in the composite would cause entanglement of MFC fibrils, and therefore compromise the enhancing effect. It was concluded that MFC was superior to BKP and MCC as reinforcement due to its higher intrinsic strength and larger aspect ratio. The reinforcing ability of MFCs cryocrushed from different sources, including kraft pulp, hemp, rutabaga, and flax, was studied (Bhatnagar and Sain 2005)—see Table 9. In a more recent study, Qiu and Netravali (2012) prepared MFC/PVA composites by film casting, and introduced chemical crosslinking between PVA and/or MFC by adding glyoxal to increase the mechanical and thermal properties of the composite. The acetyl linkages in the resulting composites were supported by FT-IR spectra, and were claimed to reduce the swellingability of PVA. Tensile tests demonstrated that crosslinking further increased the mechanical strength of composites (Table 10), whereas the TGA and DSC results showed improved thermal stability and glass transition, but reduced melting temperature and crystallinity of PVA.

Besides composites, the applications of MFC in other fields have been studied, for instance, in papermaking to enhance paper strength and improve

Table 8 Mechanical properties of microfibrillated cellulose, MFC, films and MFC-melamine formaldehyde composites (Henriksson and Berglund 2007)

Melamine formaldehyde (MF) content (wt%)	Stress at break (MPa)	Young's modulus (GPa)	Strain at break (%)
0	104	14.0	2.6
5	142	16.1	1.4
9	121	16.6	0.91
13	108	15.7	0.81

Table 9 Mechanical properties of PVA-MFC composites. MFC was produced from different sources and its volume fraction the composites was 10 % (Bhatnagar and Sain 2005)

	Tensile strength (MPa)	Modulus (GPa)
Pure PVA	69	2.29
PVA + MFC from kraft pulp	102	7.42
PVA + MFC from hemp	111	9.80
PVA + MFC from rutabaga	178	10.1
PVA + MFC from flax	76	6.10

the retention of pigment and dye (Matsuda 2000), in food as gelation agent (Funami et al. 2006), as a pharmaceutical excipient (Kumar et al. 2005), as a stabilizer in water-in-oil emulsions (Andresen and Stenius 2007), and as high absorbent material in hygiene products (Fukuda et al. 2001).

Microcrystalline cellulose

In comparison to MFC, microcrystalline cellulose (MCC) is a commercial product with over a half century of history. Interestingly, the discovery of MCC originated from a failed experiment (Battista and Smith 1962). In that experiment, Battista and Smith were trying to use a Waring Blender to disintegrate hydrolyzed cellulose in water to small particles. They thought the sharp blades of the Waring Blender would sliver off very small fragments of the agglomerated microcrystals in the hydrolyzed cellulose, and these microcrystalline fragments would settle out of water. Instead however, they obtained a stable colloidal suspension, which is known commercially as Avicel.

The production of MCC starts from acid hydrolysis of a cellulosic material, e.g. wood pulp. During the hydrolysis process, the originally tightly packed cellulose microcrystals are separated because the connecting amorphous cellulose is dissolved. These particles have a wide diameter range from 30 nm to 5 μm, and are released by mechanical disintegration. After drying, these free cellulose microcrystals aggregate again by the strong hydrogen bonds to form MCC particles with a spongy, porous, and random fine structure. An important concept during this process is the level-off degree of polymerization (LODP), which is defined as the DP of purified cellulose after hydrolysis for 15 min in 2.5 M HCl at 105 ± 1 °C. The LODP values vary from 300 to 350 for bleached ramie or hemp to 15–30 for extra high strength rayon tire cords (Battista and Smith 1962; Battista et al. 1956). Figure 9 shows two SEM images of MCC. It can be seen that the size of MCC is in the range of several micron to several tens of microns. The images also depict the morphology and structure of MCC. It can be clearly observed that MCC is the aggregation of cellulose crystallites. Since cellulose crystallites have very high strength, it is of interest to know the strength properties of MCC. This has been studied in two approaches. Edge et al. (Edge et al. 2000) investigated the strength of compacted specimens (or compacts) of MCC with median size 50 and 90 μm, respectively. The compacts were prepared by compressing MCC

Table 10 Tensile properties of PVA, MFC/PVA composites, and their glyoxal crosslinked samples

	Tensile strength (MPa)	Young's Modulus (MPa)	Fracture strain (%)
PVA	34.1 (13.3)[a]	248 (22.9)	331 (15.4)
Crosslinked PVA	47.7 (7.5)	666 (9.5)	184 (16.3)
MFC/PVA composite	53.2 (5.6)	1,033 (7.2)	25.2 (23.7)
Crosslinked MFC/PVA composite	53.7 (7.1)	1,404 (9.4)	29.6 (16.8)

The MFC contents in composites are 10 wt% (Qiu and Netravali 2012)

[a] Values in the parentheses are % coefficient of variation values

powders in a 25 mm diameter die at a load of 100 kN (200 MPa). The tensile strengths of the compacts were 11.5 ± 0.3 and 10.5 ± 0.2 MPa for the 50 and 90 μm samples, respectively. In a later study, Eichhorn and Young (2001) characterized the mechanical properties of single MCC particles using the band shift of Raman spectra, a method first reported by Hamad and Eichhorn (1997). In their experiment, MCC particles were embedded in epoxy and then a single MCC was carefully selected under the microscope. When applying forces on the cured epoxy beam, the deformation of this selected MCC particle was calculated by monitoring the shift of the band of Raman spectra at 1,095 cm^{-1}. Using this approach, the Young's modulus of MCC was estimated to be 25 ± 4 GPa.

The application of MCC in composite compounding using a variety of polymer matrices has been studied and reported. Laka et al. (2003) made MCC from wood pulp and prepared MCC/Na-carboxymethylcellulose (Na-CMC) composites by film casting of an aqueous mixture of the two compositions. The MCC used in the experiments was made from bleached wood pulp followed by grinding in a ball mill. The longitudinal size for 60 % of the particles and the transverse size for 80 % of the particles were within 3–20 μm. The testing results demonstrated that the mechanical properties of the film had no change when the MCC dry weight content was less than 43 %. However, the tensile strength and elastic modulus of the composite increased after that and reached peak values, 42 and 30 %, respectively, at 70 % MCC (dry weight) content. The authors did not give any explanation for the results. Borges et al. (Borges et al. 2004) cast MCC (Avicel) fibre-hydroxypropylcellulose (HPC) composite films from HPC acetone solution and studied their tensile properties. The MCC particles employed in their experiments had an average size of 30 μm and aspect ratio of 5. Compared to MCC-free HPC, the tensile stress and Young's modulus of the composite were increased two and three times, respectively, at 20 wt% MCC. When 1,4-butyldiisocyanate (BDI), a crosslinking agent that can react with the hydroxyl groups on HPC and MCC, was applied to film processing, maximum strength was obtained at 10 wt% MCC content and the values were 15–20 % higher than those of the un-crosslinked ones. This result was explained in terms of the improved packing of MCC in the composite films, namely better distribution, which was supported by AFM observations.

Mathew et al. (2005) prepared PLA and MCC composites by directly compounding them using a twin-screw extruder and studied the mechanical properties, crystallinity, and biodegradation of the resulting composites. The results were compared with PLA composites reinforced with wood pulp (WP) and wood flour (WF). It was demonstrated that the PLA/MCC composites performed the worst among the three types of composites (see Table 11). SEM images revealed that MCC had poor adhesion with the PLA matrix despite it being well dispersed in the composite. Compared with WP and WF, MCC had much lower aspect ratio because of its particulate form, which contributed to the poorer performance of MCC relative to other fillers. The authors also proposed the lower crystallinity of PLA/MCC composites as another possible factor accounting for the inferior mechanical properties. Degradation studies revealed that the wood flour composites have the highest degradation rate. Finally, they proposed that high performance biocomposites could be achieved if the MCC in composites could be further disintegrated into whiskers.

Petersson and Oksman (2006) prepared composites using PLA and cellulose acetate butyrate (CAB) as

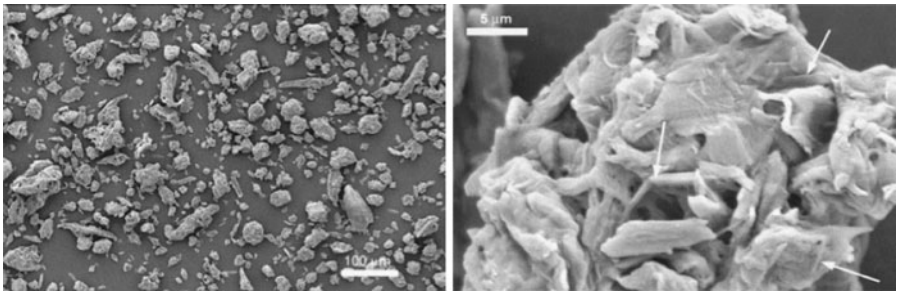

Fig. 9 SEM micrographs showing the morphology and structure of MCC. The *arrows* in the image point to cellulose crystallites in MCC particle. The *scale bars* in the images are 100 μm (*left*) and 5 μm (*right*) (Mathew et al. 2005)

Table 11 Mechanical properties of PLA and PLA composites

Composites	Tensile strength (MPa)	Elongation at break (%)	E-modulus (GPa)
PLA	49.6 ± 1	2.4 ± 0.1	3.6 ± 0.2
PLA/MCC	36.2 ± 0.9	1.7 ± 0.2	5.0 ± 0.2
PLA/WP	45.2 ± 1.3	1.9 ± 0.3	6.0 ± 0.7
PLA/WF	45.2 ± 1.3	1.7 ± 0.1	6.3 ± 0.2

For all the composites, the PLA/filler was 75/25 based on weight (Mathew et al. 2005)

Table 12 Mechanical properties of MCC composites (Petersson and Oksman 2006)

	Tensile strength (MPa)	E-modulus (GPa)	Elongation at break (%)
PLA	28.5 ± 3.8	1.7 ± 0.2	>100
PLA + 5 % MCC	31.9 ± 2.8	1.5 ± 0.2	>100
CAB	30.3 ± 2.4	0.3 ± 0.1	17
CAB + 5 % MCC	39.5 ± 3.5	0.2 ± 0.0	40

matrices. For the MCC/PLA composites, the MCC was first swollen in warm water and sonicated to loosen the MCC particles. After freeze drying, the MCC was dispersed in chloroform and sonicated again. The MCC/chloroform dispersion was then mixed with PLA/chloroform solution to cast composite films. The MCC/CAB composite films were prepared following a similar procedure, but using dimethylacetamide as the medium to disperse MCC and dissolve CAB. The mechanical properties of such films were characterized and the results are given in Table 12. The authors postulated that polymer chains could partially penetrate into MCC particles, which was supported by TEM observations. The tensile strength of these MCC composites was only slightly improved, and the elastic modulus was unaffected. The authors ascribed these results to the poor dispersion of MCC in the matrices and the presence of large MCC agglomerates.

Compounding of surface-modified MCC with PLA was also reported. Sundar et al. (2011) prepared Fe-modified MCC by reacting oxidized MCC with ferrous sulfate in NaOH solution to allow the formation of metal complex between Fe^{2+} ions and cellulose. The resulting Fe-MCC was then compounded with PLA in a brabender mixer. The authors reported that both MCC and Fe-MCC could improve the thermal stability of PLA, whereas MCC was better than Fe-MCC. The DSC results showed that the modification of MCC did not affect the glass transition and melting temperatures of PLA compared to unmodified MCC. Although there was a slight improvement in storage modulus after adding MCC and Fe-MCC in PLA, the tan δ did not change, suggesting no molecular interaction occurred between PLA and MCC. It was also found the electrical conductivity of MCC increases after Fe modification. However, the conductivity of Fe-MCC/PLA composites was not provided, despite the authors proposition that Fe-MCC was potentially suitable for conductive biopolymer composites. Furthermore, Xiao et al. (2012) modified MCC by grafting L-lactic acid oligomers and compounded it with PLA. The grafting reaction was carried out by adding MCC in L-lactic acid using $SnCl_2{\cdot}H_2O$ as the catalyst. After removing the free PLA homopolymer, the presence of grafted LA oligomer was supported by FT-IR and solid state ^{13}C NMR results. The modified MCC (g-MCC) was then compounded with PLA through melt blending followed by compression moulding to prepare g-MCC/PLA composite films. It was thus shown that surface grafting increases the compatibility of MCC with PLA, and consequently improves MCC dispersion in PLA. As a result, the g-MCC/PLA composites have much better transparency than MCC/PLA. With regard to mechanical properties, the influence of g-MCC on the storage modulus of PLA is minor, but the addition of g-MCC increases the tensile strength and strain by about 50 % compared to neat PLA at g-MCC contents of 10 and 30 wt%.

In another paper, Wu et al. (2007) prepared MCC-polyurethane (PU) composites by mixing MCC with thermoplastic PU elastomer in DMF followed by film casting. They reported the highest tensile strength of 257 MPa for the composite, at 5 wt% MCC content, compared to 39 MPa for neat PU. The strain-to-failure and Young's modulus also increased from 159 to 237 % and 4.9 to 12.9 MPa, respectively. Several factors contributed to these results. First, the MCC particles were swollen by DMF/LiCl solvent allowing the monomer to penetrate into the space within MCC, thereby increasing the adhesion at interface. Second, the hydrophilic nature of PU helps the dispersion of MCC in composites. And finally, there are hydrogen

bonds and covalent bonds formed between PU and MCC, which makes MCC not simply a filler, but a crosslinking agent in PU. Besides reinforcement, MCC can also impart other functionality to MCC/PU composites. Hatakeyama et al. (2012) prepared water absorbent MCC/PU composite foams and studied the effect of MCC particle size and content on the properties of composites. The MCC/PU composite foams were prepared by mixing all reaction ingredients under vigorous stirring and the reaction was allowed to be carried out at room temperature overnight. They reported that the apparent density of dry composites was constant regardless MCC content, whereas the apparent density of wet composites decreases with increasing MCC size and content. It was also found that MCC acted as a fast water absorbent in the composite foams, thereby reducing water adsorption time (t_s) significantly. For example, t_s is $\sim$250, $\sim$45, and $\sim$15 s for MCC/PU composite foams with 0, 5 and 20 wt% of MCC, respectively. And, since water desorption rate of the PU matrix is slower than that of MCC, then the rate of evaporation is primarily controlled by water diffusion of MCC particles in the initial stage.

Compounding of MCC with other polymeric matrices has also investigated, for example, with polypropylene (PP) (Zhang et al. 2011; Yang et al. 2011; Thummanukitcharoen et al. 2012), nylon (Kiziltas et al. 2011a), and poly(ethylene terephthalate) -poly(trimethylene terephthalate) (PET-PTT) blends (Kiziltas et al. 2011b). In general, high MCC loading is required in composites in order to improve the mechanical properties (and the contribution of MCC is normally not prominent, mainly because of its larger size compared to nano cellulosic materials, low intrinsic strength, and more importantly, low aspect ratio). It therefore remains that the primary application of MCC is in pharmaceutical production as an excipient for solid dosage forms because of its unique compressibility and carrying capacity (Fekete et al. 1998; Hileman et al. 1997; Kachrimanis and Malamataris 2004; Krogars et al. 2000; Limwong et al. 2004; Young Christopher et al. 2002). MCC compacts well under low pressure to form tablets that are hard, stable, yet disintegrate rapidly. Moreover, it is stable, safe and physiologically inert. MCC can also be used in food as a naturally derived stabilizer, texturizing agent, and fat replacer (Alexander 1992; Sakamoto 2008; Buliga et al. 1998).

Bacterial cellulose

Although plant is the most significant source of cellulose, some bacteria species can also synthesize cellulose fibres (or microbial cellulose) extracellularly, which is called bacterial cellulose (BC). BC can be synthesized from an individual bacterium, *Acetobacter xylinium (A. xylinium)* (Seidel 2004). The preparation of BC is usually conducted by culturing *A. xylinium* in Hestrin–Schramm medium statically for several days at around 30 °C. When the bacteria grow in the medium, they extrude glucan chains, which aggregate into microfibrils. The microfibrils finally bundle to form microbial cellulose ribbons. BC harvested from the culture medium need to be purified by washing with alkaline solution and water extensively. As shown in Fig. 10, BC has a network structure, which is in the form of pellicle made up of a random assembly of ribbon shaped fibrils. The diameter of the fibrils is less than 100 nm, containing a bundle of much finer microfibrils.

BC consists of long, entangled spaghetti-like fibres. The fine fibrillar structure has high purity, and comprises dimensionally uniform cellulose fibril bundles, which impart BC with high strength. Hsieh et al. (2008) used a Raman spectroscopic technique to measure the strength of a single BC filament. They reported that the Young's modulus of BC filament was 114 GPa, which is much higher than those of MFC and

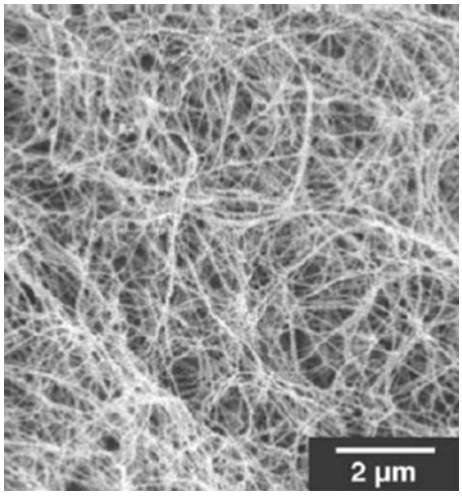

Fig. 10 SEM micrograph of bacterial cellulose (Nakagaito et al. 2005)

MCC. Guhados et al. (2005) reported the value of 78 ± 17 GPa measured directly using an atomic force microscope (AFM). Yamanaka et al. (1989) investigated the strength of BC sheets. The processing conditions of their BC sheets varied from air-dried to hot-pressed at a temperature range from 20 to 200 °C. The results showed that the Young's modulus of BC sheets was >15 GPa and was not affected by the variation of processing conditions.

BC can, in principle, grow on a variety of substrates with almost any shape. This characteristic is very useful for making biocompatible materials for applications in tissue engineering (Chen et al. 2007; Luo et al. 2008). Nevertheless, a problem that limits the application of BC is its low yield. Krystynowicz et al. (2002) studied the factors that affect BC yield, including agitation, aeration, and culture media composition. For instance, BC yield varied between 0.48 and 5.35 g/l after 14 days of culture. The long culture time, the expensive culturing media, and tedious post-treatment significantly increase the production cost of BC.

BC can, however, be incorporated with other biocompatible materials to form a suitable tissue engineering material. Millon and Wan (2006) reported that polyvinyl alcohol (PVA)/BC composites could be prepared by applying freeze–thaw cycles on PVA/BC mixtures in water. By testing the stress–strain properties of these PVA/BC composites, they found that the properties of the composites could be tuned by changing the composition to match those of the porcine aorta and the aortic heart valve—with a potential to be used for tissue replacement. Luo et al. (2008) reported the preparation of collagen/BC composites by adding collagen to the culture medium of *A. xylinium*. The SEM results demonstrated that this composite had different micromorphology as its nanofibrils are more porous than pristine BC, which means the collagen/BC composite has larger surface area. Therefore, it has the potential application as tissue engineering scaffolds, because the large surface area is beneficial for cellular attachment and vascularisation.

Efforts were also made to prepare BC composites with high strength. Nakagaito et al. (2005; Nakagaito and Yano 2004) studied the mechanical properties of phenolic resin/BC composites and compared the results with phenolic resin/MFC composites. Phenolic resin/BC composites were prepared by impregnating BC sheets in phenolic resin followed by compression at 100 MPa. It was found that BC composites are stronger than MFC composites: Young's modulus increased from 19 to 28 GPa, while the bending strength increased from 370 to 425 MPa. The higher strength of BC composites was ascribed to the fine, pure, and dimensionally uniform cellulose fibril bundles. However, considering the long process and cost of preparing the composites, the extent of the strength improvement is not economical in practice.

BC sheets treated with alkaline and/or oxidative solutions have measured values of Young's modulus (E) and sound propagation velocity (C) of 30 GPa and 5,000 m/s, respectively. These values are much higher than that of ordinary cone paper ($E = 1.5$ GPa, $C = 1{,}600$ m/s). However, unlike the other materials with high E and C', which are typically metallic materials, BC has good damping properties and, therefore, the potential to be used as acoustic materials (Nishi et al. 1990).

Shah and Brown (2005) reported the idea to make electronic paper displays using BC. The first experimental step was to dope various conductors into BC sheets by using impregnation solutions which increased the conductivity of BC by orders of magnitude. In the next step, a suitable electrochromic dye was embedded in BC sheets. The dyes can undergo optical changes upon the application of an electric charge by a reversible redox reaction. Finally, a single-pixel device is fabricated using the sheet so that it can be scaled up to full-scale multipurpose displays. This type of display promises paper-like reflectivity, flexibility, contrast, and biodegradability. Marins et al. (2011) prepared conductive nanocomposites by in situ polymerization of aniline in the presence of hydrated BC sheets. They doped the polyaniline (Pani) with dodecylbenzene sulfonic acid (DBSA) and found the optimum DBSA/aniline molar ratio is 1.5, where the resulting nanocomposite had higher bulk conductivity. This type of nanocomposites has potential applications in optical and electrical displays.

Since BC microfibrils are less than 50 nm in cross section, which is smaller than one-tenth of the visible light wavelength (400–800 nm), they do not cause light scattering (Beecroft and Ober 1997). This feature is used to prepare optically transparent nanocomposite films reinforced with BC. Yano et al. (2005) prepared transparent BC based nanocomposite films by impregnating BC sheets into acrylic or epoxy resin. The

transmittance of their nanocomposite films was about 80–90 % in the visible light range, or had less than 10 % loss compared to neat resin films. BC-reinforced nanocomposite films are flexible, transparent, and dimensionally stable under heating. Retegi et al. (2012) have recently used epoxidized soy-bean oil (ESO) as the matrix and impregnated it into BC films in THF. The BC nanofibre surface was modified via acetylation before mixing to improve compatibility—a critical factor for transparency. According to the authors, an ESO/BC nanocomposite film with 75 wt% BC still possessed about 60 % of the degree of transparency through wavelength range 400–1,100 nm. By comparison, the degree of transparency for ESO and BC films were 75 and 18 % (the maximum value at 1,000 nm wavelength), respectively. Another investigation by Ummartyotin et al. (2012) deals with the fabrication of organic light emitting diode (OLED) using polyurethane (PU)/BC nanocomposite film as substrate. Ummartyotin et al. (2012) impregnated BC films in PU resin to prepare PU/BC nanocomposites with 10–50 wt% fibre content. The resulting PU/BC nanocomposite films demonstrated high transmittance in the range 75–87 % of visible light. Other attributes of PU/BC nanocomposite films include flexibility, dimensional stability, and thermal stability. The authors then used these PU/BC films as substrates to fabricate an organic light emitting diode (OLED), which could emit light when bent.

Evans et al. (2003) studied the potential application of BC for fuel cells. They found that BC possesses reducing groups capable of catalyzing the precipitation of palladium from aqueous solution within its structure to generate a high surface area with catalytic ability. Since BC can be dried to form a thin membrane, it is suitable for the construction of membrane electrode assemblies (MEAs). Their experiments showed that palladium-BC can catalyze the generation of hydrogen when incubated with sodium dithionite and can generate an electrical current from hydrogen in an MEA. This technique may have a promising future in fuel cell development.

Cellulose nanocrystals (CNC)

Cellulose nanocrystals (CNC), also referred to as nanocrystalline cellulose (NCC) (Khan et al. 2012; Huq et al. 2012), cellulose nanowhiskers (CNW) (Dufresne 2000) or cellulose crystallites (Revol et al. 1994), are extracted from wood or non-wood biomass by chemically removing lignin, hemicellulose, and the amorphous cellulose regions. Cellulose in plants is biosynthesized to form long, slender monocrystalline fibrils, within which the cellulose molecules are arranged parallel to one another with a twofold screw symmetry along their length (Frey-Wyssling 1954). The cellulose chains in the fibrils are bundled laterally by intra- and inter-molecular hydrogen bonds. As these cellulose fibrils are very pure and have few defects, they have a high elastic modulus close to the theoretical value of a perfect cellulose crystal, which is 150 GPa (Sakurada and Nukushina 1962).

CNC is prepared by hydrolysis of cellulosic biomass, for instance wood pulp, in mineral acid (sulfuric or hydrochloric), a process first proposed by Rånby over half a century ago (Rånby 1951, 1952). The preparation process starts with milling the pulp to uniform small particle size, followed by acid hydrolysis of the cellulose raw material to remove any polysaccharide bonded on the cellulose fibril surface and the amorphous or disordered portion of cellulose, which separates the fibrils (Revol et al. 1992). The hydrolysis is then terminated by rapid dilution of the acid, followed by acid removal via centrifugation and/or dialysis. Mechanical forces, e.g. sonication, are applied to break up the aggregation of cellulose fibrils to obtain a suspension of CNC. Since most of the non-cellulose and amorphous portion of cellulose are removed during hydrolysis, CNC has high crystallinity (90 % or greater) (Guo and Catchmark 2012). Other than wood pulp, CNC has been prepared from a variety of sources, such as MCC (Araki et al. 1999), sugar beet (Dinand et al. 1999), cotton (Dong et al. 1998), tunicate (Samir et al. 2004b), potato peel (Chen et al. 2012), and wheat straw (Dufresne et al. 1997; Helbert et al. 1996). The typical physical dimensions of CNC vary with the raw material source. Some examples are: (3–5) $\times$ 180 $\pm$ 75 nm for bleached softwood kraft pulp (Araki et al. 1998), 7 $\times$ (100–300) nm for cotton (Dong et al. 1998), 20 $\times$ (100–2,000) nm for *Valonia* (Imai et al. 1998), 10 $\times$ 410 $\pm$ 181 nm (Chen et al. 2012), and (10–20) nm $\times$ (100 nm–several μm) for tunicate cellulose (Favier et al. 1995b). Figure 11 shows the appearance of CNC from different sources.

Šturcová et al. (2005) measured the elastic modulus of CNC particles—extracted from tunicate—using a Raman spectroscopic technique and reported axial

modulus to be 143 GPa. Atomic force microscopy (AFM) was also employed to characterize individual CNC crystals. Iwamoto et al. (2009) deposited CNC (from tunicate) on a specially designed silicon wafer with grooves 227 nm in width and carried out a three-point bending test using AFM cantilever. They reported elastic modulus values of 145.2 ± 31.3 and 150.7 ± 28.8 GPa for single CNC crystals obtained through TEMPO-oxidation and acid hydrolysis of tunicate, respectively. Moreover, Lahiji et al. (2010) measured the transverse elastic modulus (E_T) of CNC crystals extracted from wood using AFM. They developed a procedure using the force-distance data from fully 3D finite element methods of tip-CNC indentation and obtained E_T values of 18–50 GPa in dry nitrogen.

CNC is not soluble in many organic solvents, but can form colloidal suspensions in water. The stability of the suspensions depends on the dimensions of crystallites, the size polydispersity, and the surface charge. It was reported that CNC prepared by sulfuric acid hydrolysis can form more stable suspensions than those obtained from hydrochloric acid hydrolysis, because the former produces negatively-charged crystallites through the sulfate esters introduced during hydrolysis (Araki et al. 1998). The surface sulfate ester content of CNC can be quantified by conductometric titration against diluted sodium hydroxide or elemental analysis (Abitbol et al. 2013). If the concentration is high enough, well dispersed CNC suspensions have birefringent domains when observed through two crossed polarizers (Fig. 12) (Marchessault et al. 1959). It was also found that CNC could form a chiral nematic-ordered phase above a critical concentration (Revol et al. 1992). Again, the ability to form such a phase is dependent on the acid employed for the

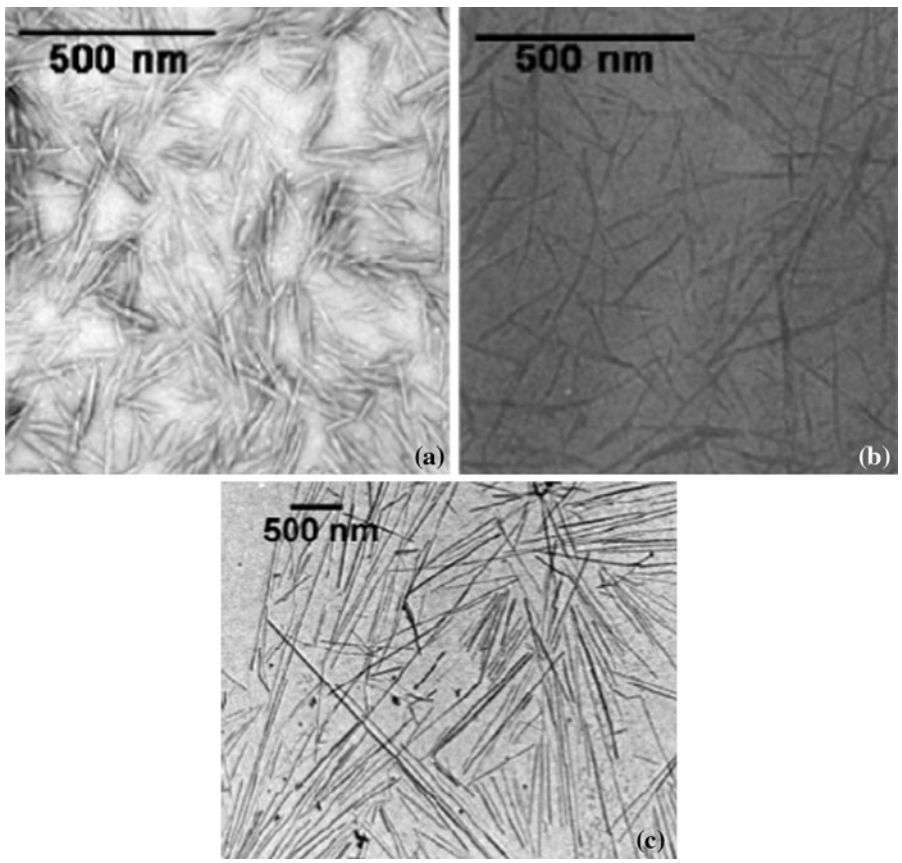

Fig. 11 TEM images of CNC from different sources. **a** Cotton, **b** sugar-beet pulp, and **c** tunicin (the cellulose extracted from tunicate, a sea animal) (Samir et al. 2005a)

Fig. 12 CNC suspension shows birefringence between crossed polarizers (Petersson et al. 2007)

hydrolysis. CNC hydrolyzed in sulfuric acid and phosphoric acid has the chiral nematic phase, whereas that hydrolyzed using hydrochloric acid does not (Revol et al. 1998). The ability to disperse CNC in solvents, other than water, was investigated by van den Berg et al. (2007). They dispersed lyophilized CNC in various polar solvents at a concentration of 1 mg/mL and the dispersability of CNC was judged by the presence of birefringence or not. They checked CNC hydrolyzed in sulfuric acid and hydrochloric acid and the results are summarized in Table 13. However, as shown in the table, some samples needed extensive ultrasonication to facilitate the dispersion, which resulted in damage to the structure of CNC. The authors performed TEM image analysis to show that the length of CNC decreased from 2.20 ± 0.20 μm (as-prepared) to 0.63 ± 0.05 μm (lyophilized and processed from *N*-methyl pyrrolidone) and 1.61 ± 0.16 μm (lyophilized and processed from formic acid). Another important finding was that the negative charge obtained by sulfuric acid hydrolysis was very important for the dispersibility of CNC.

Although CNC produced by sulfuric acid hydrolysis has better stability in water because of the negative charge, it was found that the sulfate groups introduced during hydrolysis can compromise the thermal stability of CNC (Roman and Winter 2004). Usually, the higher sulfate groups content in cellulose, the lower the temperature of cellulose thermal degradation. Wang et al. (2007) reported that the thermal stability of CNC can be improved by neutralizing the acid sulfate groups with NaOH solution.

Table 13 Dispersability of lyophilized CNCs in polar solvents (van den Berg et al. 2007)

Solvent	CNC-SO_4	CNC-HCl
Water	++	−
N,*N*-dimethyl formamide	+	−
Dimethyl sulfoxide	+	−
N-methyl pyrrolidone	++	−
Formic acid	++	++
m-cresol	++	++

++ = Dispersed after sonication 6 h or less. + = Dispersed after sonication 24 h (72 h in the case of *N*,*N*-dimethyl formamide) at ca. 60 °C. − = Did not disperse

One major application of CNC is reinforcement in composites. CNC is of interest in composite research for two main reasons: the high strength imparted by their almost perfect crystal structure and the high specific surface area due to their nano-scale size. Numerous contributions in this field have been made (Ljungberg et al. 2005, 2006; Chauve et al. 2005; Samir et al. 2004a, b; Dufresne 2003; Bonini et al. 2002; Mathew and Dufresne 2002; Angles and Dufresne 2000, 2001; Angles et al. 2000b; Bonini et al. 2000; Dufresne et al. 1997, 1999; Favier et al. 1997; Elazzouzi et al. 2006; Eichhorn 2011; Habibi et al. 2010; Dufresne 2000) after Favier et al. (1995a) first reported on the reinforcing effect of CNC in nanocomposites.

Significant efforts in this field have been focusing on the preparation methods of CNC nanocomposites, i.e., how to effectively disperse CNC in polymer matrices and provide good interface between reinforcement and matrix. Cellulosic materials are hydrophilic, which makes them difficult to disperse well in hydrophobic thermoplastics. This problem is worsened for nano-scale cellulose crystallites, because their large specific surface area, or high surface energy, promotes aggregation. In general, there are two approaches to incorporate CNC into a polymeric matrix: before the formation of polymer chains, i.e., in situ polymerization, or via post-polymerization compounding.

The preparation of CNC-based nanocomposites by in situ polymerization is typically carried out in a solvent, in which the monomers are soluble, and CNC dispersible, in the solvent. For instance, the polymerization of acrylamide (AM) (Zhou et al. 2011b;

Table 14 Tensile properties of CNC/PLA composites containing a surfactant (Bondeson and Oksman 2007a)

Material	Tensile strength (MPa)	Tensile modulus (GPa)	Elongation at break (%)
PLA	62.8 ± 1.0	2.65 ± 0.08	19.5 ± 9.7
PLA + 5 %CNC	55.5 ± 2.9	2.69 ± 0.2	9.7 ± 0.9
PLA + 5 %CNC + 5 %S	52.4 ± 0.4	3.10 ± 0.15	3.1 ± 0.2
PLA + 5 %CNC + 10 %S	45.7 ± 0.9	2.36 ± 0.13	20.5 ± 7.1
PLA + 5 %CNC + 20 %S	23.5 ± 0.5	1.15 ± 0.03	>100

The "S" in the sample IDs denotes the surfactant

Yang et al. 2013) and acrylic acid (AA) (Yang et al. 2012) in water and diisocyanates and diols in dimethylformamide (DMF) (Pei et al. 2011). The dispersion of CNC rods almost has no disturbance through the polymerization course, and the formation of CNC percolation network potentially leads to significant improvements in mechanical property. On the other hand, the presence of CNC can change the gelation behaviour of the specific polymerization system by the formation of a percolated network and/or a crosslinking reaction between monomers and CNC, which may consequently require longer time to complete the polymerization reaction. It is apposite to note, that using organic solvents can introduce further complications to the polymerization process.

Compared to in situ polymerization, post-polymerization compounding is more widely used and studied. The most direct method is to use water as the processing medium to compound CNC with polymers (Samir et al. 2004c, 2005b; Angles et al. 2000a). However, this restricts the choice of polymer matrices to those that are water soluble. Another approach has used latexes of hydrophobic polymers mixed with CNC aqueous suspensions to obtain homogeneous composites (Dufresne et al. 1999; Ruiz et al. 2001; Hajji et al. 1996). As described above, lyophilized CNC can be dispersed in an organic solvent with the assistance of strong sonification (Samir et al. 2004b; van den Berg et al. 2007). Polymers can then be introduced in the organic solvent. All of these methods use film casting as the route to form CNC containing composites. However, film casting is inefficient in large scale production, which restricts the potential applications of these approaches. Other ways to disperse CNC in a hydrophobic medium are to modify the CNC surface physically or chemically, for example, applying a large amount of surfactant (Petersson et al. 2007; Bondeson and Oksman 2007a). However, the amount of surfactant required to cover the CNC surface is high, and could undermine the properties of the resulting composite. For instance, Bondeson and Oksman (2007a) used Beycostat A B09, an anionic surfactant of acid phosphate ester of ethoxylated nonylphenol, to improve the dispersion of CNC in a PLA matrix. The freeze-dried CNC, surfactant, and PLA were compounded using a twin screw extruder. In their experiments, the content of the CNC was fixed at 5 wt% in the composites, whereas the dosage of the surfactant increased from 0 to 20 wt%. The tensile strength results of the composites are listed in Table 14, and it can be seen from the table that the addition of surfactants compromises the strength of the composites.

Modification of CNC surfaces is one of the most extensively studied areas in the field. Besides adding surfactants, other reported methods include grafting of small molecules (Yuan et al. 2006; Gousse et al. 2002; Oliveira Taipina et al. 2013; Shang et al. 2013), grafting of polymers (Ljungberg et al. 2005; Lin et al. 2009), oxidation (Araki et al. 2001; Habibi et al. 2006).[5] Dispersion—throughout the reaction and purification processes—is a key challenge when dealing with CNC, or other nanomaterial, surface modification. Beside conventional polymer processing methods, e.g., casting, co-extrusion, and melt blending, Capadona et al. (2007) reported an approach to form a three-dimensional template via self-assembly of well dispersed CNC rods, followed by filling the template with a polymer to create a strong and flexible nanocomposite. Other, different approaches have been used for preparing CNC-polymer nanocomposites, such as electrospinning (Dong et al. 2012; Xiang et al. 2013; Zhou et al. 2011a) and layer-by-layer self-assembly (Li et al. 2013).

Processing methods have a significant effect on the properties of CNC-reinforced nanocomposites. Hajji

[5] The chemistry of CNC modification bears similarities to the methods used on macroscale cellulosic materials, which is reviewed in the previous section.

et al. (1996) studied the effect of preparation methods on the mechanical properties of a CNC-based nanocomposite. The matrix polymer used in their experiments was a latex copolymer comprising 66 wt% of butyl acrylate, 33 wt% of styrene, and 1 wt% of acrylic acid. CNC was compounded with the matrix by directly mixing CNC suspensions with the latex. Three types of processing methods were used to prepare composite films: (1) casting by direct water evaporation (E), (2) freeze drying followed by hot pressing (HP), and (3) freeze drying, then extruding followed by hot pressing (XP). The tensile strength of the films was tested at 23 °C, above the glass transition temperature of the matrix polymer (~0 °C), and are given in Table 15. Of all the three methods, the composite film prepared by water evaporation gives the best mechanical performance, probably because this method had less influence on the orientation of CNC, provides better dispersion of CNC in matrices, and causes less damage to the CNC structure. These results clearly show the importance of processing methods and uniform dispersion of the reinforcement in the matrix on composite properties.

There are four main factors that affect the mechanical properties of CNC nanocomposites. The first, and most critical, is compatibility of CNC and polymer resin. This is essential to allow smooth and uniform dispersion of reinforcement into the matrix, and avoid CNC aggregation. It is particularly significant in large-scale polymer processing techniques, like extrusion and compression/injection moulding. The second factor is the molecular structure of the matrix, which influences the interaction between matrix and CNC and their interfacial properties. The third is the aspect ratio of CNC particles, which is determined by the origin of the cellulose source and the preparation conditions. Typically, a higher aspect ratio gives more reinforcement potential, assuming aggregation does not occur. The fourth factor is the composite preparation method. The importance of this factor is supported by the results in Table 15.

Classical composite theory requires that the matrix/filler interaction must be stronger than the filler/filler interaction to obtain high performance composites. With CNC-based nanocomposites however, an opposite trend has been observed in several experiments (Angles and Dufresne 2001; Dufresne et al. 1999; Grunert and Winter 2002; Nair et al. 2003). For example, Nair et al. (2003) prepared natural rubber nanocomposites reinforced with crab shell chitin whiskers by solution casting and studied the effect of chemical modification on the whiskers. In their experiments, different chemical coupling agents were tested, including phenyl isocyanate (PI), alkenyl succinic anhydride (ASA), and 3-isopropenyl-α,α′-dimethylbenzyl isocyanate (TMI). After modification, the whiskers were dispersed in toluene and then mixed with natural rubber toluene solution. The toluene was evaporated to obtain nanocomposites. Since the surface of modified whiskers became more hydrophobic—confirmed by contact angle measurement, the whisker-matrix interactions were improved by the modification. However, DMA results (Fig. 13) demonstrated that the nanocomposites reinforced with modified whiskers were inferior to that filled by the unmodified one. The reason is that the surface modification interrupts the interaction among whiskers, which is critical for the formation of the three-dimensional network of chitin whiskers, required by percolation theory.

The Halpin–Kardos model—introduced in the previous section of this review—can be applied to predict the composite strength of CNC reinforced polymer composites. It was found that the modulus calculated using this model agreed well with the experimental data when the testing temperature was

Table 15 Mechanical properties of CNC based nanocomposites processed by different methods (Hajji et al. 1996)

CNC content (wt%)	E		HP		XP	
	Modulus (MPa)	Tensile strength (MPa)	Modulus (MPa)	Tensile strength (MPa)	Modulus (MPa)	Tensile strength (MPa)
0	0.2	0.15	0.2	0.12	0.2	0.12
1	0.6	0.49	0.5	0.31	0.4	0.23
6	32.3	5.00	5.2	1.63	1.5	1.06

E = solution casting, HP = freeze drying followed by hot compression, and XP = freeze drying, extrusion and hot compression

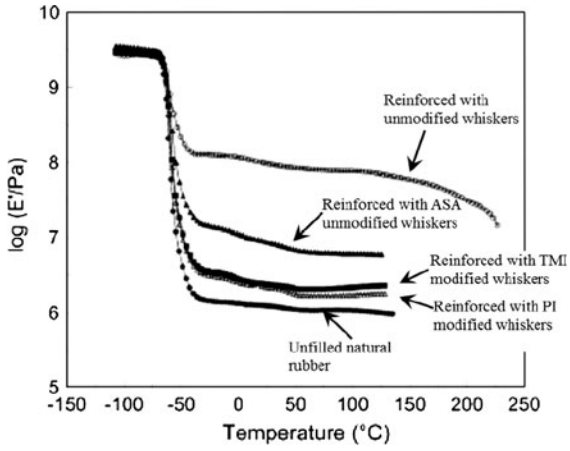

Fig. 13 Storage tensile modulus versus temperature tested at 1 Hz for chitin whiskers/natural rubber nanocomposites (Nair et al. 2003)

below glass transition (T_g) of the matrices (Chazeau et al. 1999; Favier et al. 1995a; Dufresne et al. 1997; Hajji et al. 1996; Helbert et al. 1996). However, in the rubbery state of the matrices, the observed increase in modulus was much higher than could be reached through reinforcement by discrete particles. Taking into account the high specific surface area and the numerous hydroxyl groups available on CNC, it was highly likely that hydrogen bonds could form between the CNC particles, which cause the development of a CNC network. Therefore, it would be reasonable to consider the critical assumption in the Halpin–Kardos model of no interaction between filler particles as being inapplicable in these cases. This conclusion led researchers to apply percolation theory to analyze CNC nanocomposites. Percolation is a statistical theory that can be used in any system involving a great number of particles likely to be connected (Hammersley 1957). In such a system, there is a threshold volume fraction dividing the system into two states, in which the species are either individual or connected. According to this theory, it is the rigid network formed by the CNC in nanocomposites that is responsible for the significant strength improvement at temperatures above T_g. Percolation modelling therefore consists of three main steps: (1) calculation of the percolation threshold; (2) estimation of the modulus of the percolation reinforcement network; and (3) model construction. The simplest series–parallel model has two parallel phases, which involve three parts: the matrix; the percolating network of reinforcement; and the non-percolating reinforcement. Their relationships can schematically be illustrated in Fig. 14.

Based on these, Ouali et al. (1991) proposed that the elastic tensile modulus E_C of the composites can be calculated by:

$$E_C = \frac{(1-2\psi+\psi v_R)E_S E_R + (1-v_R)\psi E_R^2}{(1-v_R)E_R + (v_R-\psi)E_S}$$

where the subscripts S and R refer to the soft and rigid phases, and v_R is the volume fraction of the rigid phase. The percolating fraction of the rigid phase ψ can be written as:

$$\psi = 0 \qquad for\ v_R < v_{Rc}$$
$$\psi = v_R\left(\frac{v_R - v_{Rc}}{1-v_{Rc}}\right)^b \qquad for\ v_R > v_{Rc}$$

where v_{Rc} is the percolation threshold, and b is the critical percolation exponent, which equals 0.4 for a 3D network (Stauffer 1985; De Gennes 1979). Above T_g, the modulus of the matrix is much lower than that of the rigid phase. Thus, the equation can be rewritten as

$$E_C = \psi E_R$$

It was found that this model fits the experimental results well, especially for high filler loading (Stauffer 1985; De Gennes 1979). For example, Favier et al. (1995a; Dubief et al. 1999; Dufresne et al. 1997, 1999; Hajji et al. 1996) used DMA to study the mechanical properties of a series of nanocomposites consisting of latex of styrene and butyl acrylate copolymer ($T_g \sim 0$ °C) and different contents of CNC. The shear modulus of the composites against temperature is given in Fig. 15. For temperatures below T_g, CNC only shows a limited contribution to the modulus. When the temperature increases to T_g, the mechanical properties of the neat copolymer drop drastically,

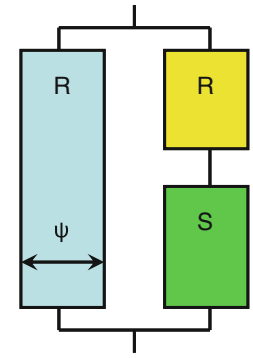

Fig. 14 Schematic diagram of the series–parallel model. R and S represent the rigid phase (reinforcement) and the soft phase (polymer matrices), respectively, and ψ is the volume fraction of the percolating rigid phase

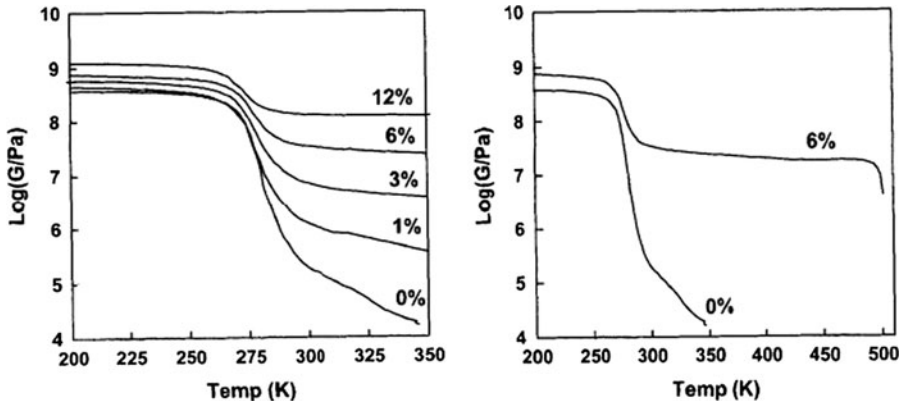

Fig. 15 The logarithm of the shear modulus of the CNC reinforced nanocomposite as a function of temperature. The *graph* on the *left* shows the reinforcing effect of CNC at different CNC content. The *graph* on the *right* demonstrates the improvement of thermal stability. The *numbers* in the *plots* are the CNC contents by weight percentage (Favier et al. 1997)

while the nanocomposites show little decrease of modulus. At temperatures above T_g, the nanocomposites exhibit almost constant modulus over a wide temperature range. The shear modulus of the nanocomposite containing 12 wt% CNC is 4 orders of magnitude higher than that of the neat matrix copolymer at 350 K. For the sample containing 6 wt% CNC, the high modulus can be retained up to 500 K, the temperature around which cellulose starts to degrade.

The authors then used these data to fit models as shown in Fig. 16. It can be seen that the modulus calculated according to the Halpin–Kardos model does not fit experimental results at all, while the percolation model is in good agreement with them, especially for higher CNC contents. For the discrepancy between experimental results and the percolation modeling at low CNC content, a possible explanation is that the calculation assumes a monodisperse CNC size distribution.

Percolation theory is well demonstrated in a paper on the development of stimuli-responsive CNC reinforced poly(ethylene oxide-co-epichlorohydrin) (EO-EPI) (Fig. 17) nanocomposite (Capadona et al. 2008). The CNC employed in their experiments was extracted from tunicates with an aspect ratio of 84. The nanocomposites were prepared using a template method described above (Capadona et al. 2007). As EO-EPI has a T_g around −37 °C, it is in the rubbery phase at room temperature. The authors found that the mechanical properties of the CNC-(EO-EPI) nanocomposites could be simply switched by swelling them with water. That is to say, when the composites were dry, they demonstrated high strength at 25 °C and the results could be fitted by the percolation model. However, when the composite

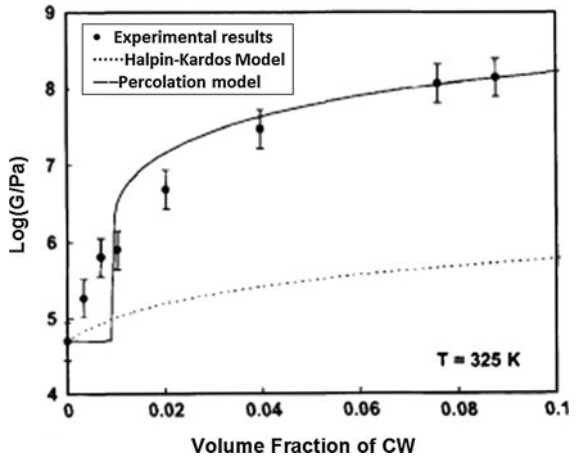

Fig. 16 Comparison of experimental values and the results calculated by Halpin–Kardos model and percolation model respectively. The values are taken at 325 K (Favier et al. 1997)

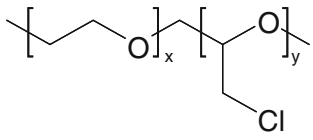

Fig. 17 Chemical structure of poly(ethylene oxide-co-epichlorohydrin) (EO-EPI)

took up 30 % v/v water, the storage modulus dropped drastically and the results matched the value calculated from the Halpin–Kardos model. Moreover, the strength of the swollen composites could be restored by drying again—see Fig. 18. To exclude the possibility that these changes were caused by the plasticizing of EO-EPI by water, the authors used another solvent, isopropanol (IPA), which can swell the nanocomposites to similar levels as water. The

nanocomposites swollen by IPA exhibited high strength fitting the percolation model. It was concluded that the property changes of the nanocomposites were ascribed to the formation or breaking of hydrogen bonds among the CNC particles. Under dry conditions, the numerous hydrogen bonds among CNC particles make them form a percolated network, thereby greatly enhancing the strength of the nanocomposite. When water is introduced, the formed hydrogen bonds are disrupted by the water molecules, and the CNC particles affect the nanocomposite's strength individually rather than as a network. These results demonstrate the mechanism that enhances the performance of nanocomposites and the importance of a percolated network.

All-cellulose composites

A new class of composites solely based on cellulosic contents, referred to as all-cellulose composites (ACCs), attracted serious attention arguably a decade ago (see, for instance, Nishino et al. 2004). ACCs have one chemical component—cellulose; however, the constituents usually have different morphological and/or structural characteristics, in contrast to the commonly used definition for composites, i.e., a material

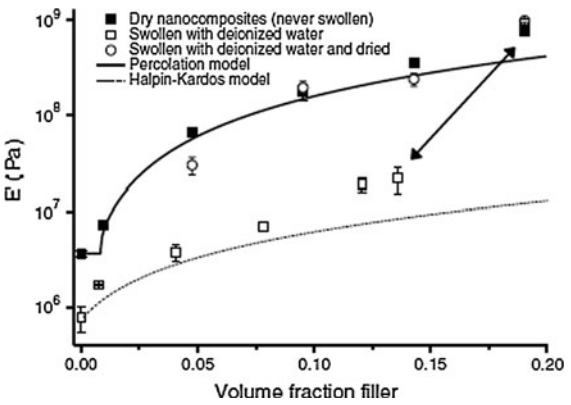

Fig. 18 Tensile storage moduli E′ of CNC-(EO-EPI) nanocomposites as a function of volume fraction of CNC. The nanocomposites were conditioned by either drying in vacuum, equilibrium swelling in deionized water, or swelling to saturation in deionized water followed by redrying in vacuum. The *lines* represent values predicted by the percolation and Halpin–Kardos models. The *arrow* indicates changes in modulus and volume fraction of CNC resulting from aqueous swelling of one selected sample (19 % v/v CNC) (Capadona et al. 2007)

comprising two distinct constituents with distinct physico-chemical properties leading new synergetic properties and/or functionalities—see first section of this review for more details. Theoretically, this can help mitigate, or overcome, compatibility issues between reinforcement and matrix.

There are two typical strategies for the preparation of ACCs reported in the literature: two-step and one-step methods (Fig. 19). In the two-step method, first reported by Nishino et al. (2004), a portion of cellulose is initially dissolved in a solvent, followed by regeneration of the cellulose in the presence of another undissolved cellulose component. Kraft pulp was dissolved in a solvent and then regenerated in the presence of ramie fibres (Nishino et al. 2004). More recently, this method was further developed for use of cellulose derivatives as the dissolved portion in the first step. For example, Vallejos et al. (2012) prepared ACCs by electrospinning cellulose acetate (CA) solution with dispersed cellulose nanocrystals (CNC) to produce precursor CA/CNC composites. The CA component in precursor composites was then converted to regenerated cellulose via alkaline hydrolysis to obtain ACCs. In the one-step method, however, cellulosic fibers are partially dissolved in a solvent and then regenerated in situ to form a matrix around the undissolved portion. Gindl and Keckes (2005) were first to demonstrate the efficacy of this method by preparing ACC films via partial dissolution of microcrystalline cellulose powder followed by casting. The properties of the resulting ACC films could be tuned by adjusting the ratio of cellulose I and II.

There is a variety of solvents that have the ability to dissolve cellulose, however, three of the more common ones used in the preparation of ACCs include lithium chloride/*N*,*N*-dimethylacetamide (LiCl/DMAc), NaOH aqueous solution with additives, and ionic liquids (ILs). Attempts have been made to use a mixture of LiCl and DMAc [(LiCl) = 8 wt%] as the solvent of choice for ACC preparation (Nishino et al. 2004; Gindl and Keckes 2005; Gindl et al. 2006b; Nishino and Arimoto 2007; Qin et al. 2008; Duchemin et al. 2009; Pullawan et al. 2010, 2012; Yousefi et al. 2011a). Cellulose can be dissolved in LiCl/DMAc by directly adding it to the mixture, or by mixing cellulose with DMAc first followed by LiCl. An activation process is required in either approach in order to efficiently and fully dissolve cellulose (Turbak et al. 1981). As such, LiCl salts can form intermediate complexes with cellulose, thereby

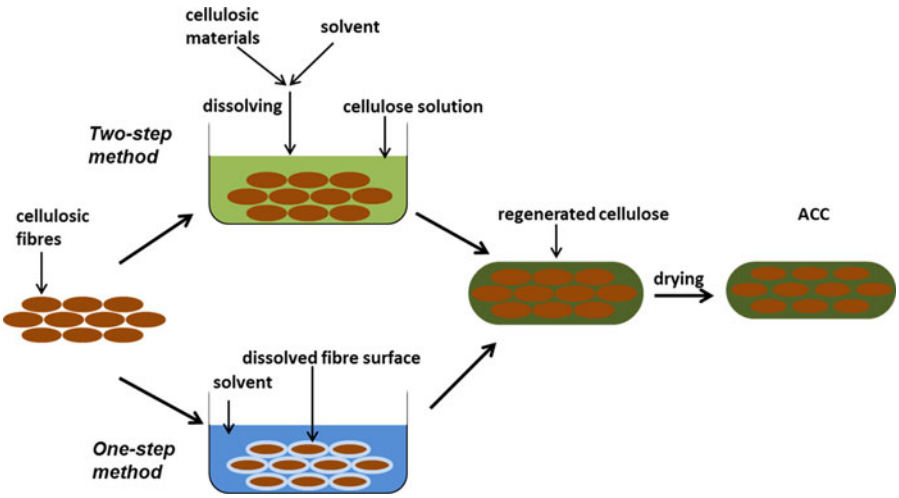

Fig. 19 Schematic representation of the two-step (*top*) and one-step (*bottom*) preparation methods of ACCs

reducing the hydrogen bond effect between the cellulose molecules (Jing et al. 2007), and the activation process-controlled selective dissolution of cellulose is therefore the primary reason for the application of LiCl/DMAc in ACCs preparation.

Another route for the dissolution of cellulose is the use of NaOH aqueous solution with the addition of urea (Qi et al. 2009; Yang et al. 2010; Wang and Chen 2011) or poly(ethylene glycol) (PEG) (Han and Yan 2010). The solutions require cooling to sub-zero temperature, ca. −12 to −15 °C, with active stirring in order to dissolve the cellulose. Upon returning to room temperature, the non-dissolved cellulose portion is introduced into the solution, and selective dissolution is realized. The dissolved cellulose is regenerated from the solution using a coagulation bath of diluted H_2SO_4, or by removing NaOH and additives using water.

Yet another widely used solvent in ACC preparation is ionic liquids (ILs) (Zhao et al. 2009; Ma et al. 2011; Yousefi et al. 2011b; Huber et al. 2012a, c). ILs are molten salts with melting points below 100 °C, and were recognized as effective solvents for cellulose almost eight decades ago (Graenacher 1934). There are numerous possible combinations of a wide variety of cations and anions, while the most successful ILs to dissolve cellulose are hydrophilic and consist of methylimidazoloium or methylpyridinium cation cores with allyl-, ethyl-, or butyl-side chains combined with chloride, acetate, or formate anions (Huber et al. 2012b). The ILs' ability to dissolve cellulose originates from their high effective polarity, due to their ionic character. ILs possess some attractive properties as a processing solvent, including negligible vapor pressure, ease of recycling (low cost), thermal stability, capability for rapid and complete dissolution of a broad range of cellulose sources and with no requirement for pre-treatment or activation (Swatloski et al. 2002). From the available possible routes, ILs are therefore potentially effective green solvents. However, some serious studies have found some ILs to be toxic and hazardous to environment (Swatloski et al. 2003; Thuy Pham et al. 2010).

Cellulose regeneration is a critical step in ACC preparation as it determines the final phase of cellulose matrix. It is normally carried out by removing the solvent using a coagulant, e.g., water and alcohol, followed by removal of the coagulant by drying. Duchemin et al. (2009) studied the structure–property relationships of ACCs, and found that ACCs with slow precipitation rate possessed better mechanical properties owing to the higher crystallinity of the cellulose matrix. This is likely due to the fact that the dissolved cellulose chains have more time to (re)order themselves into a lower energy configuration in such conditions.

Many different cellulosic materials have been employed to prepare ACCs. For example, MCC (Pullawan et al. 2010), wood pulp (Nishino et al. 2004), and filter paper (Zhao et al. 2009) were used for matrix, while the reinforcement included CNC (Qi et al. 2009), ramie fiber (Qin et al. 2008), rice husks (Zhao et al. 2009), and rayon fibers (Huber et al.

2012a). Together with the choice of suitable processing method and solvent system, the different combinations of cellulosic constituents can help generate a fairly wide range of properties. It is thus hard to provide an effective comparison by simply examining the mechanical properties of resulting ACCs; however, there are some general trends that can be summarized. Soykeabkaew et al. (2008) prepared ACCs with ramie fibers using the one-step method and found the mechanical properties to be strongly dependent on the dissolution time—namely, the longitudinal tensile strength decreases with increasing dissolution time, whereas the transverse tensile strength follows an opposite trend. This likely stems from reduction of the cross-sectional area of the load-bearing cellulose fibers with increasing dissolution time; meanwhile the volume fraction of the matrix increased and the interfacial adhesion between cellulose fibers and matrix improved. Figure 20 shows typical SEM images of ACC cross-sections, which illustrate changes occurring in fiber-matrix interfaces as a function of dissolution time. As such, ACC processing conditions can finely be tuned to produce desired properties.

Processing conditions notwithstanding, researchers have explored other treatments to improve the mechanical properties of ACCs. Qin et al. (2008) prepared ACCs using ramie fibers via the two-step method and treated the ACCs with alkali solution, or mercerization. They found that the tensile strength of mercerized ACCs was improved from 15 to 95 % depending on the composition of the ACCs. The authors ascribed the improvement to the removal of voids and cracks in ACCs brought on by the treatment (Qin et al. 2008). Gindl et al. (2006a, b) studied the crystallites of ACCs when applying a wet-drawing force, and found that the cellulose crystallites tend to orient with their crystallographic *c*-axis parallel to the force direction and an irreversible preferred orientation is induced—orientation changes linearly with applied strain and is independent of the actual stress. Meanwhile, the overall crystallinity of the composite stays unaffected. Pullawan et al. (2012) prepared CNC-reinforced ACCs and manipulated the orientation of CNC rods in the composites by applying a strong magnetic field during composite casting. The magnetic alignment is driven by the characteristic negative diamagnetic anisotropy of the CNC. However, the results showed that the presence a magnetic field only induced the CNC rods to be partially oriented, which was ascribed to the lack of freedom to rotate within the composite. It was also found that lowering the volume fraction of CNC allowed easier manipulation of the orientation of CNC rods, thus leading to a relatively larger increase in ACC stiffness and strength. The authors further indicated that different domains were formed in the resulting ACC, where CNC rods were oriented in some locale and randomly distributed in others. This could be explained by the competition between maximizing entropy by randomly oriented CNC rods and the effect of the magnetic field. Meanwhile, the application of the magnetic field only led to inducing negligible orientation of the matrix (Pullawan et al. 2012).

As alluded to above, comparisons of the mechanical properties of different ACCs is, strictly speaking,

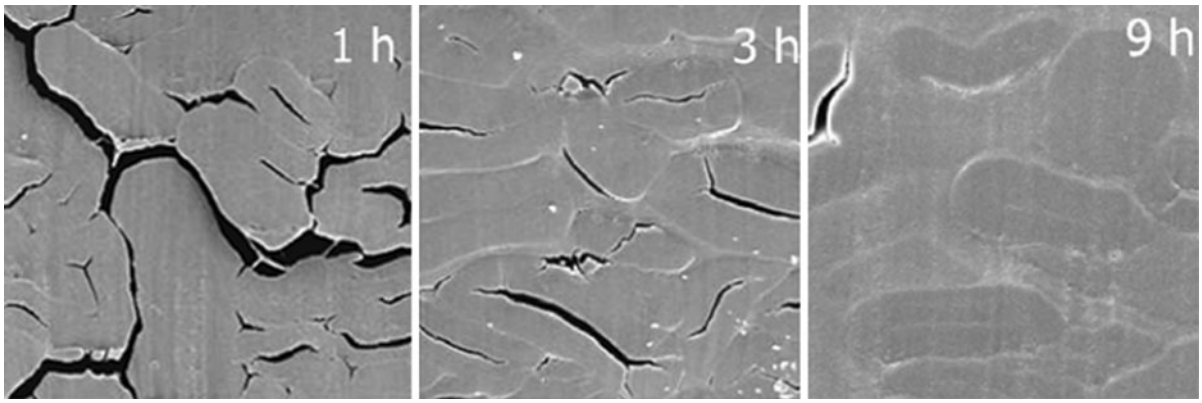

Fig. 20 SEM images of ACC cross-sections indicating changes in the interfacial phenomena as dissolution time increases (Soykeabkaew et al. 2008)

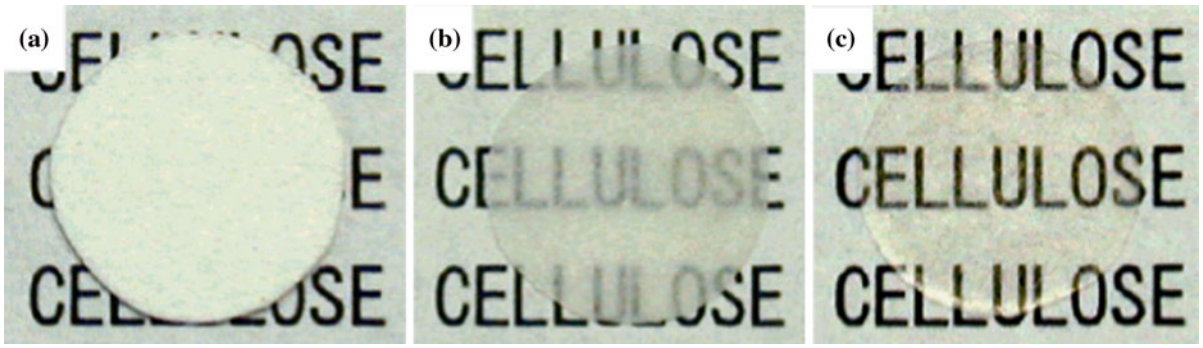

Fig. 21 Optical photographs showing transparency of **a** filter paper and ACCs with **b** 6 h and **c** 12 h dissolution times, respectively (Nishino and Arimoto 2007)

challenging owing to the multitude of processing and functional attributes to be considered. Nonetheless, one can make some stringent comparisons between performance trends of ACCs relative to, for instance, cellulose-reinforced polymers, such as PLA, PCL, PHB, PP, etc. One such comparative study has recently been made by Huber et al. (2012b), where they methodically examined the tensile strength and stiffness in a large selection of ACCs prepared by either of the previously described (one-step or two-step) methods using different reinforcements (CNC, MCC, pulp fiber, ramie fiber, etc.) relative to the performance of random or unidirectional cellulose-reinforced thermoplastic or thermoset resins. Their detailed comparisons showed the tensile strength and stiffness of ACCs to be favorably comparable to the overwhelming majority of synthetic composites—in certain cases significantly higher (Huber et al. 2012b).

As with bacterial cellulose (Yano et al. 2005), owing to its small cross-sectional dimensions, ACCs could prove ideal for the preparation of optically transparent nanocomposites (Gindl and Keckes 2005; Nishino and Arimoto 2007; Soykeabkaew et al. 2008; Yousefi et al. 2011b). The one-step method was employed by these research groups, where it was discovered the transparency of the ACCs increased with increasing dissolution time. Figure 21 depicts an example of the change in transparency of ACCs with dissolution time, which indicates that better transparency emanates from (1) more effective interface between reinforcement and matrix, (2) closure of internal pores, and (3) reduced surface roughness (Nishino and Arimoto 2007; Soykeabkaew et al. 2008; Yousefi et al. 2011b).

Promising potential of all-cellulose nanocomposites notwithstanding, there remain serious processing challenges and fundamental analysis to be further explored. One pressing issue is the effect of hydrophilicity on ACC processing and end-use performance. Inherent cellulose hydrophobicity causes swelling of the composite and rapid performance deterioration under longterm exposure to external load. Furthermore, cellulose swelling also takes place during ACC processing, leading to (unfavorable) shrinkage of the composite after drying. Moreover, while it is recognized that compatibility of the components is not an issue, careful quantitative evaluation of the interface in ACCs needs critical and in-depth examination in order to comment on the durability or fatigue performance of ACCs. This is essential if ACCs are to prove promising for automotive and other applications, where exposure to sustained external loading under different environments is critical.

Summary and concluding remarks

Lignocellulosic fibers consist of concentric composite layers of cellulose fibrils embedded into an amorphous matrix of hemicellulose and lignin. Hydrolytic processes can be used to hydrolyse the hemicellulose and amorphous cellulose leaving highly crystalline cellulose nanocrystals (CNC). Microcrystalline cellulose (MCC) is produced through an established process that employs hydrochloric acid hydrolysis, as opposed to sulfuric acid hydrolysis in the case of CNC. If mechanical and/or enzymatic treatment is applied to wood pulp fibres, a fine network of microfibrillated

cellulose (MFC) can however be produced. Microfibrillar bundles of cellulose, or bacterial cellulose (BC), can be extracellularly synthesized by some bacterial species.

MFC, MCC, BC, and CNC have similar chemical constituents, but very different physical and solid-state properties—refer to Table 16. Because of its nano-size, CNC has a large surface area ($\sim$400 m^2/g), and has conductive properties. It also has a chiral nematic structure rendering CNC capable of producing unique optical properties, and has high strength approaching that of pure cellulose owing to CNC's high degree of crystallinity (>90 %). However, the high degree of self-affinity, nano-scale, and hydrophobicity render CNC compatibilization and dispersion in polymer systems of great import and challenge. Cost and scalability are two critical components in these considerations. By comparison, MCC is a micro-scale material, and as such its physical and mechanical properties, as well as the challenges they present, are different to that of CNC. The involved preparation process and low yield of BC restrict its wide application. The web-like structure and hydrophobicity of MFC/NFC similarly present challenges to dispersion in, and compatibility with, polymeric matrices using conventional polymer processing techniques.

Micro- and nano-scaled cellulosic materials therefore possess the potential to act as high-performance reinforcement in polymeric composites, thereby creating opportunities to develop high-tenacity and highly-durable engineering materials from a renewable resource suitable for consumer, structural and medical applications. To date, the potential of BC, MCC, CNC and MFC/NFC reinforced nanocomposites has only primarily been realized in composites prepared either by film casting or by template impregnation. The challenge, however, for R&D over the next years is to translate the successful potential of micro/nano-cellulosic reinforcement to commercially available polymer processing techniques (e.g., extrusion, injection-molding) through the development of cost-effective, scalable compatibilization and dispersion techniques.

Last, but not least, all-cellulose composites (ACCs) are monocomponent materials, forming an emerging class of biomaterials that can be produced from a broad variety of possible cellulosic raw materials. Appropriate use of solvents and processing methods

Table 16 Typical physical properties of microfibrillated cellulose (MFC), microcrystalline cellulose (MCC), and nanocrystalline cellulose (CNC)

	Morphology	Diameter (nm)	Aspect ratio	Modulus (GPa)	Specific surface area (m^2/g)
MFC	Network	15–1,000[a]	15–100[b]	10–13[c]/29–36[d]	$\sim$7[e]/29–202[f]
MCC	Particulate	1,000–100,000[g]	<5[h]	5–9[i]/$\sim$25[j]	$\sim$1–20[k]
CNC	Rod or whisker	2–20[l]	$\sim$1–100[l]	143–150[m]	400[n]

[a] Measured on individual fibrils (Henriksson et al. 2007; Turbak et al. 1983; Chakraborty et al. 2005)

[b] Measured on individual fibrils (Henriksson et al. 2007, 2008; Chakraborty et al. 2005)

[c] Measured on MFC sheets by tensile test (Henriksson et al. 2008)

[d] Measured on individual fibrils (Tanpichai et al. 2012a)

[e] BET analysis on lyophilized MFC (Lu et al. 2008)

[f] Determined on MFC suspensions by Congo red adsorption method (Spence et al. 2010)

[g] From references (Mathew et al. 2005; Luukkonen et al. 1999; Borges et al. 2004; Ardizzone et al. 1999)

[h] From reference (Borges et al. 2004)

[i] Measured on compressed bulk MCC (Hancock et al. 2000)

[j] Measured on individual MCC particles by following the shift of the Raman-sensitive band(s) with increasing applied strain (Eichhorn and Young 2004)

[k] From reference (Luukkonen et al. 1999)

[l] From reference (Samir et al. 2005a)

[m] From references (Šturcová et al. 2005; Iwamoto et al. 2009; Sakurada and Nukushina 1962)

[n] Unpublished results from the authors' laboratory based on SEM evaluation of approximately 1,000 samples

offers promising opportunities to manufacture ACCs with tailored properties for a multitude of applications ranging from barrier materials to automotive parts.

Acknowledgments The authors gratefully acknowledge financial support from Natural Resources Canada under the Tranformative Technology program, and critical commentary on this review by Dr Richard Berry, Mr Thanh Trung and the anonymous reviewers of this journal.

References

Abitbol T, Kloser E, Gray DG (2013) Estimation of the surface sulfur content of cellulose nanocrystals prepared by sulfuric acid hydrolysis. Cellulose 20(2):785–794

Adusumalli R-B, Reifferscheid M, Weber H, Roeder T, Sixta H, Gindl W (2006) Mechanical properties of regenerated cellulose fibres for composites. Macromol Symp 244(1):119–125

Alam MK, Khan MA, Lehmann EH, Vontobel P (2007) Study of the water uptake and internal defects of jute-reinforced polymer composites with a digital neutron radiography technique. J Appl Polym Sci 105(4):1958–1963

Alexander RJ (1992) Carbohydrates used as fat replacers. In: Alexander RJ, Zobel HE (eds) Developments in carbohydrate chemistry. Am. Assoc. Cereal Chem, St. Paul, MN, pp 343–370

Andresen M, Stenius P (2007) Water-in-oil emulsions stabilized by hydrophobized microfibrillated cellulose. J Dispersion Sci Technol 28(6):837–844

Angelini LG, Lazzeri A, Levita G, Fontanelli D, Bozzi C (2000) Ramie (*Boehmeria nivea* (L.) Gaud.) and Spanish Broom (*Spartium junceum* L.) fibres for composite materials: agronomical aspects, morphology and mechanical properties. Ind Crops Prod 11(2–3):145–161

Angles MN, Dufresne A (2000) Plasticized starch/tunicin whiskers nanocomposites. 1. Structural analysis. Macromolecules 33(22):8344–8353

Angles MN, Dufresne A (2001) Plasticized starch/tunicin whiskers nanocomposite materials. 2. Mechanical behavior. Macromolecules 34(9):2921–2931

Angles MN, Vignon MR, Dufresne A (2000a) Plasticized starch and cellulose whiskers composites. Mater Tech 88(7–8):59–61

Angles MN, Vignon MR, Dufresne A (2000b) Plasticized starch and cellulose whiskers composites. Mater Tech (Paris) 88(7–8):59–61

Araki J, Wada M, Kuga S, Okano T (1998) Flow properties of microcrystalline cellulose suspension prepared by acid treatment of native cellulose. Colloids Surf A 142(1):75–82

Araki J, Wada M, Kuga S, Okano T (1999) Influence of surface charge on viscosity behavior of cellulose microcrystal suspension. J Wood Sci 45(3):258–261

Araki J, Wada M, Kuga S (2001) Steric stabilization of a cellulose microcrystal suspension by poly(ethylene glycol) grafting. Langmuir 17(1):21–27

Ardizzone S, Dioguardi FS, Mussini T, Mussini PR, Rondinini S, Vercelli B, Vertova A (1999) Microcrystalline cellulose powders: structure, surface features and water sorption capbility. Cellulose 6:57

Augier L, Sperone G, Vaca-Garcia C, Borredon ME (2007) Influence of the wood fibre filler on the internal recycling of poly (vinyl chloride)-based composites. Polym Degrad Stab 92(7):1169–1176

Bailie C (2005) Green composites: polymer composites and the environment. CRC Press, Boca Raton, FL

Bataille P, Dufourd M, Sapieha S (1994) Copolymerization of styrene onto cellulose activated by corona. Polym Int 34(4):387–391

Battista OA, Smith PA (1962) Microcrystalline cellulose. J Ind Eng Chem 54(9):20

Battista OA, Coppick S, Howsmon JA, Morehead FF, Sisson WA (1956) Level-off degree of polymerization. Relation to polyphase structure of cellulose fibers. J Ind Eng Chem 48:333

Beecroft LL, Ober CK (1997) Nanocomposite materials for optical applications. Chem Mater 9(6):1302–1317

Beg MDH, Pickering KL, Weal SJ (2005) Corn gluten meal as a biodegradable matrix material in wood fibre reinforced composites. Mater Sci Eng, A 412(1–2):7–11

Belgacem MN, Gandini A (2005a) Surface modification of cellulose fibres. Polim Cienc Tecnol 15(2):114–121

Belgacem MN, Gandini A (2005b) The surface modification of cellulose fibres for use as reinforcing elements in composite materials. Compos Interfaces 12(1–2):41–75

Benerito RR, Ward TL, Soignet DM, Hinojosa O (1981) Modifications of cotton cellulose surfaces by use of radiofrequency cold plasmas and characterization of surface changes by ESCA. Text Res J 51(4):224–232

Bhatnagar A, Sain M (2005) Processing of cellulose nanofiber-reinforced composites. J Reinf Plast Compos 24(12): 1259–1268

Bisanda ETN, Ansell MP (1992) Properties of sisal-CNSL composites. J Mater Sci 27(6):1690–1700

Bledzki AK, Faruk O (2006a) Influence of processing temperature on microcellular injection-moulded wood-polypropylene composites. Macromol Mater Eng 291(10):1226–1232

Bledzki AK, Faruk O (2006b) Microcellular wood fibre reinforced PP composites: a comparative study between extrusion, injection moulding and compression moulding. Int Polym Process 21(3):256–262

Bledzki AK, Gassan J (1999) Composites reinforced with cellulose based fibres. Prog Polym Sci 24(2):221–274

Bledzki AK, Reihmane S, Gassan J (1996) Properties and modification methods for vegetable fibers for natural fiber composites. J Appl Polym Sci 59(8):1329–1336

Bledzki AK, Faruk O, Sperber VE (2006) Cars from bio-fibers. Macromol Mater Eng 291(5):449–457

Boissard CIR, Bourban P-E, Plummer CJG, Neagu RC, Månson J-AE (2012) Cellular biocomposites from polylactide and microfibrillated cellulose. J Cell Plast 48(5):445–458

Boldizar A, Klason C, Kubat J, Naeslund P, Saha P (1987) Prehydrolyzed cellulose as reinforcing filler for thermoplastics. Int J Polym Mater 11(4):229–262

Bondeson D, Oksman K (2007a) Dispersion and characteristics of surfactant modified cellulose whiskers nanocomposites. Compos Interfaces 14(7–9):617–630

Bondeson D, Oksman K (2007b) Polylactic acid/cellulose whisker nanocomposites modified by polyvinyl alcohol. Compos A 38(12):2486–2492

Bonini C, Heux L, Cavaille J-Y (2000) Polypropylene reinforced with cellulose whiskers. Mater Tech 88(7–8):55–58
Bonini C, Heux L, Cavaille J-Y, Lindner P, Dewhurst C, Terech P (2002) Rodlike cellulose whiskers coated with surfactant: a small-angle neutron scattering characterization. Langmuir 18(8):3311–3314
Borges JP, Godinho MH, Martins AF, Stamatialis DF, De Pinho MN, Belgacem MN (2004) Tensile properties of cellulose fiber reinforced hydroxypropylcellulose films. Polym Compos 25(1):102–110
Bos HL, Van den Oever MJA (1999) The large influence of flax fiber structure on composite strength. Paper presented at the international conference on woodfiber-plastic composites, 5th, Madison, WI, United States, May 26–27, 1999
Bos HL, Molenveld K, Teunissen W, van Wingerde AM, van Delft DRV (2004) Compressive behaviour of unidirectional flax fibre reinforced composites. J Mater Sci 39(6): 2159–2168
Botaro VR, dos Santos CG, Arantes Junior G, da Costa AR (2001) Chemical modification of lignocellulosic materials by irradiation with Nd-YAG pulsed laser. Appl Surf Sci 183(1–2):120–125
Boufi S, Gandini A (2001) Formation of polymeric films on cellulosic surfaces by admicellar polymerization. Cellulose 8(4):303–312
Buliga GS, Tuason DC Jr, Venables AC (1998) Microcrystalline cellulose-containing texture and stabilizer composition for food. WO Patent 9833394
Capadona JR, Van Den Berg O, Capadona LA, Schroeter M, Rowan SJ, Tyler DJ, Weder C (2007) A versatile approach for the processing of polymer nanocomposites with self-assembled nanofibre templates. Nat Nanotechnol 2(12):765–769
Capadona JR, Shanmuganathan K, Tyler DJ, Rowan SJ, Weder C (2008) Stimuli-responsive polymer nanocomposites inspired by the sea cucumber dermis. Science 319(5868):1370
Carlsson CMG, Ström G (1991) Reduction and oxidation of cellulose surfaces by means of cold plasma. Langmuir 7(11):2492–2497
Castellano M, Gandini A, Fabbri P, Belgacem MN (2004) Modification of cellulose fibers with organosilanes: under what conditions does coupling occur? J Colloid Interface Sci 273(2):505–511
Chakraborty A, Sain M, Kortschot M (2005) Cellulose microfibrils: a novel method of preparation using high shear refining and cryocrushing. Holzforschung 59:102–107
Chakraborty A, Sain M, Kortschot M (2006) Reinforcing potential of wood pulp-derived microfibres in a PVA matrix. Holzforschung 60(1):53–58
Chauve G, Heux L, Arouini R, Mazeau K (2005) Cellulose poly(ethylene-co-vinyl acetate) nanocomposites studied by molecular modeling and mechanical spectroscopy. Biomacromolecules 6(4):2025–2031
Chazeau L, Cavaille JY, Canova G, Dendievel R, Boutherin B (1999) Viscoelastic properties of plasticized PVC reinforced with cellulose whiskers. J Appl Polym Sci 71(11):1797–1808
Chen H-L, Porter RS (1994) Composite of polyethylene and kenaf, a natural cellulose fiber. J Appl Polym Sci 54(11): 1781–1783
Chen J, Tsubokawa N (2000) Electric properties of conducting composite from poly(ethylene oxide) and poly(ethylene oxide)-grafted carbon black in solvent vapor. Polym J 32(9):729–736
Chen YM, Gong JP, Osada Y (2007) Gel: a potential material as artificial soft tissue. Macromol Eng 4:2689–2717
Chen D, Lawton D, Thompson MR, Liu Q (2012) Biocomposites reinforced with cellulose nanocrystals derived from potato peel waste. Carbohydr Polym 90(1):709–716
Clarke AR, Archenhold G, Davidson NC (1995) A novel technique for determining the 3D spatial distribution of glass fibres in polymer composites. Compos Sci Technol 55(1): 75–91
Datta C, Basu D, Roy A, Banerjee A (2004) Mechanical and dynamic mechanical studies of epoxy/VAc-EHA/HMMM IPN-jute composite systems. J Appl Polym Sci 91(2): 958–963
De Gennes PG (1979) Scaling concepts in polymer physics. Cornell University Press, Ithaca, NY
De SK, Murty VM (1984) Short fiber-rubber composites. Polym Eng Rev 4(4):313–343
Dikobe DG, Luyt AS (2007) Effect of poly (ethylene-co-glycidyl methacrylate) compatibilizer content on the morphology and physical properties of ethylene vinyl acetate-wood fiber composites. J Appl Polym Sci 104(5):3206–3213
Dinand E, Chanzy H, Vignon MR (1999) Suspensions of cellulose microfibrils from sugar beet pulp. Food Hydrocolloids 13(3):275–283
Doan T–T-L, Gao S-L, Maeder E (2006) Jute/polypropylene composites I. Effect of matrix modification. Compos Sci Technol 66(7–8):952–963
Dong XM, Revol J-F, Gray DG (1998) Effect of microcrystallite preparation conditions on the formation of colloid crystals of cellulose. Cellulose 5(1):19–32
Dong H, Strawhecker KE, Snyder JF, Orlicki JA, Reiner RS, Rudie AW (2012) Cellulose nanocrystals as a reinforcing material for electrospun poly(methyl methacrylate) fibers: formation, properties and nanomechanical characterization. Carbohydr Polym 87(4):2488–2495
Duanmu J, Gamstedt EK, Rosling A (2007) Synthesis and preparation of crosslinked allylglycidyl ether-modified starch-wood fibre composites. Starch 59:523–532
Dubief D, Samain E, Dufresne A (1999) Polysaccharide microcrystals reinforced amorphous poly (β-hydroxyoctanoate) nanocomposite materials. Macromolecules 32(18): 5765–5771
Duchemin BJC, Newman RH, Staiger MP (2009) Structure-property relationship of all-cellulose composites. Compos Sci Technol 69(7–8):1225–1230
Dufresne A (2000) Dynamic mechanical analysis of the interphase in bacterial polyester/cellulose whiskers natural composites. Compos Interfaces 7(1):53–67
Dufresne A (2003) Interfacial phenomena in nanocomposites based on polysaccharide nanocrystals. Compos Interfaces 10(4–5):369–387
Dufresne A, Cavaille J-Y, Helbert W (1997) Thermoplastic nanocomposites filled with wheat straw cellulose whiskers. Part II: effect of processing and modeling. Polym Compos 18(2):198–210
Dufresne A, Kellerhals MB, Witholt B (1999) Transcrystallization in Mcl-PHAs/cellulose whiskers composites. Macromolecules 32(22):7396–7401

Edge S, Steele DF, Chen A, Tobyn MJ, Staniforth JN (2000) The mechanical properties of compacts of microcrystalline cellulose and silicified microcrystalline cellulose. Int J Pharm 200(1):67–72

Eichhorn SJ (2011) Cellulose nanowhiskers: promising materials for advanced applications. Soft Matter 7(2):303–315

Eichhorn SJ, Young RJ (2001) The Young's modulus of a microcrystalline cellulose. Cellulose 8(3):197–207

Eichhorn SJ, Young RJ (2004) Composite micromechanics of hemp fibres and epoxy resin microdroplets. Compos Sci Technol 64(5):767–772

Elazzouzi S, Nishiyama Y, Putaux J-L, Paintrand I, Schmutz M, Heux L (2006) Chiral nematic suspensions of cellulose whiskers in water and in organic solvents. Paper presented at the 231st ACS National Meeting, Atlanta, GA, United States

Evans BR, O'Neill HM, Malyvanh VP, Lee I, Woodward J (2003) Palladium-bacterial cellulose membranes for fuel cells. Biosens Bioelectron 18(7):917–923

Favier V, Canova GR, Cavaille JY, Chanzy H, Dufresne A, Gauthier C (1995a) Nanocomposite materials from latex and cellulose whiskers. Polym Adv Technol 6(5):351–355

Favier V, Chanzy H, Cavaille JY (1995b) Polymer nanocomposites reinforced by cellulose whiskers. Macromolecules 28(18):6365–6367

Favier V, Canova GR, Shrivastava SC, Cavaille JY (1997) Mechanical percolation in cellulose whisker nanocomposites. Polym Eng Sci 37(10):1732–1739

Fedullo N, Sorlier E, Sclavons M, Bailly C, Lefebvre JM, Devaux J (2007) Polymer-based nanocomposites: overview, applications and perspectives. Prog Org Coat 58(2–3):87–95

Fekete R, Zelko R, Marton S, Racz I (1998) Effect of the formulation parameters on the characteristics of pellets. Drug Dev Ind Pharm 24(11):1073–1076

Felix J, Gatenholm P, Schreiber HP (1994) Plasma modification of cellulose fibers: effects on some polymer composite properties. J Appl Polym Sci 51(2):285–295

Fink HP, Weigel P, Purz HJ, Ganster J (2001) Structure formation of regenerated cellulose materials from NMMO-solutions. Prog Polym Sci 26(9):1473–1524

Forgacs OL (1963) The characterization of mechanical pulps. Pulp Paper Mag Can 64(C):T89

Frey-Wyssling A (1954) The fine structure of cellulose microfibrils. Science 119:80

Frone AN, Panaitescu DM, Donescu D, Spataru CI, Radovici C, Trusca R, Somoghi R (2011) Preparation and characterization of PVA composites with cellulose nanofibers obtained by ultrasonication. BioRes 6(1):487–512

Fukuda S, Takahashi M, Yuyama M, Oka N (2001) Incontinence pads using highly absorbent sheets. JP Patent 2001340369

Funami T, Kishimoto K, Tsutsumino T (2006) Food gels for distribution at normal temperature. JP Patent 2006212006

Fung CP (2004) Fibre orientation of fibre-reinforced PBT composites in injection moulding. Plast, Rubber Compos 33(4):170–176

Gindl W, Keckes J (2005) All-cellulose nanocomposite. Polymer 46(23):10221–10225

Gindl W, Martinschitz KJ, Boesecke P, Keckes J (2006a) Changes in the molecular orientation and tensile properties of uniaxially drawn cellulose films. Biomacromolecules 7(11):3146–3150

Gindl W, Martinschitz KJ, Boesecke P, Keckes J (2006b) Structural changes during tensile testing of an all-cellulose composite by in situ synchrotron X-ray diffraction. Compos Sci Technol 66(15):2639–2647

Gousse C, Chanzy H, Excoffier G, Soubeyrand L, Fleury E (2002) Stable suspensions of partially silylated cellulose whiskers dispersed in organic solvents. Polymer 43(9):2645–2651

Graenacher C (1934) Cellulose solution. US Patent 1943176

Grishanov SA, Harwood RJ, Booth I (2006) A method of estimating the single flax fibre fineness using data from the LaserScan system. Ind Crops Prod 23(3):273–287

Grunert M, Winter WT (2002) Nanocomposites of cellulose acetate butyrate reinforced with cellulose nanocrystals. J Polym Environ 10(1/2):27–30

Guhados G, Wan W, Hutter JL (2005) Measurement of the elastic modulus of single bacterial cellulose fibers using atomic force microscopy. Langmuir 21(14):6642–6646

Guo J, Catchmark JM (2012) Surface area and porosity of acid hydrolyzed cellulose nanowhiskers and cellulose produced by *Gluconacetobacter xylinus*. Carbohydr Polym 87(2):1026–1037

Habibi Y, Chanzy H, Vignon M (2006) TEMPO-mediated surface oxidation of cellulose whiskers. Cellulose 13(6):679–687

Habibi Y, Lucia LA, Rojas OJ (2010) Cellulose nanocrystals: chemistry, self-assembly, and applications. Chem Rev 110(6):3479–3500

Hajji P, Cavaille JY, Favier V, Gauthier C, Vigier G (1996) Tensile behavior of nanocomposites from latex and cellulose whiskers. Polym Compos 17(4):612–619

Halpin JC, Kardos JL (1972) Moduli of crystalline polymers employing composite theory. J Appl Phys 43(5):2235–2241

Hamad WY (2002) Cellulosic materials-fibers, networks and composites. Kluwer Academic Publishers, Massachusetts

Hamad WY, Eichhorn S (1997) Deformation micromechanics of regenerated cellulose fibers using Raman spectroscopy. J Eng Mater Technol 119(3):309–313

Hammersley JM (1957) Percolation processes. II. The connective constant. Proc Camb Philol Soc 53:642–645

Han D, Yan L (2010) Preparation of all-cellulose composite by selective dissolving of cellulose surface in PEG/NaOH aqueous solution. Carbohydr Polym 79(3):614–619

Hancock BC, Clas SD, Christensen K (2000) Micro-scale measurement of the mechanical properties of compressed pharmaceutical powders. 1: the elasticity and fracture behavior of microcrystalline cellulose. Int J Pharm 209(1–2):27–35

Hatakeyama H, Kato N, Nanbo T, Hatakeyama T (2012) Water absorbent polyurethane composites derived from molasses and lignin filled with microcrystalline cellulose. J Mater Sci 47(20):7254–7261

Helbert W, Cavaille JY, Dufresne A (1996) Thermoplastic nanocomposites filled with wheat straw cellulose whiskers. Part I: processing and mechanical behavior. Polym Compos 17(4):604–611

Henriksson M, Berglund LA (2007) Structure and properties of cellulose nanocomposite films containing melamine formaldehyde. J Appl Polym Sci 106(4):2817–2824

Henriksson M, Henriksson G, Berglund LA, Lindstroem T (2007) An environmentally friendly method for enzyme-

assisted preparation of microfibrillated cellulose (MFC) nanofibers. Eur Polym J 43(8):3434–3441
Henriksson M, Berglund LA, Isaksson P, Lindstroem T, Nishino T (2008) Cellulose nanopaper structures of high toughness. Biomacromolecules 9(6):1579–1585
Hileman GA, Upadrashta SM, Neau SH (1997) Drug solubility effects on predicting optimum conditions for extrusion and spheronization of pellets. Pharm Dev Technol 2(1):43–52
Hokens D, Mohanty AK, Misra M, Drzal LT (2002) The influence of surface modification and compatibilization on the performance of natural fiber reinforced biodegradable thermoplastic composite. Polymer Prepr 43(1):482–483
Hristov V, Vlachopoulos J (2007) Influence of coupling agents on melt flow behavior of natural fiber composites. Macromol Mater Eng 292(5):608–619
Hsieh YC, Yano H, Nogi M, Eichhorn SJ (2008) An estimation of the Young's modulus of bacterial cellulose filaments. Cellulose 15(4):507–513
Huber T, Bickerton S, Müssig J, Pang S, Staiger MP (2012a) Solvent infusion processing of all-cellulose composite materials. Carbohydr Polym 90(1):730–733
Huber T, Mössig J, Curnow O, Pang S, Bickerton S, Staiger M (2012b) A critical review of all-cellulose composites. J Mater Sci 47(3):1171–1186
Huber T, Pang S, Staiger MP (2012c) All-cellulose composite laminates. Compos A 43(10):1738–1745
Huda MS, Drzal LT, Misra M, Mohanty AK (2006) Wood-fiber-reinforced poly (lactic acid) composites: evaluation of the physicomechanical and morphological properties. J Appl Polym Sci 102(5):4856–4869
Hull D, Clyne TW (1996) An introduction to composite materials. Cambridge University Press, Cambridge
Huq T, Salmieri S, Khan A, Khan RA, Le Tien C, Riedl B, Fraschini C, Bouchard J, Uribe-Calderon J, Kamal MR, Lacroix M (2012) Nanocrystalline cellulose (NCC) reinforced alginate based biodegradable nanocomposite film. Carbohydr Polym 90(4):1757–1763
Idicula M, Boudenne A, Umadevi L, Ibos L, Candau Y, Thomas S (2006) Thermophysical properties of natural fibre reinforced polyester composites. Compos Sci Technol 66(15):2719–2725
Imai T, Boisset C, Samejima M, Igarashi K, Sugiyama J (1998) Unidirectional processive action of cellobiohydrolase Cel7A on Valonia cellulose microcrystals. FEBS Lett 432(3): 113–116
Iwamoto S, Kai W, Isogai A, Iwata T (2009) Elastic modulus of single cellulose microfibrils from tunicate measured by atomic force microscopy. Biomacromolecues 10(9):2571–2576
Iwatake A, Nogi M, Yano H (2008) Cellulose nanofiber-reinforced polylactic acid. Compos Sci Technol 68(9):2103–2106
Jing H, Liu Z, Li H-y, Wang G-h, Pu J-w (2007) Solubility of wood-cellulose in LiCl/DMAC solvent system. For Stud China 9(3):217–220
Joly C, Kofman M, Gauthier R (1996) Polypropylene/cellulosic fiber composites: chemical treatment of the cellulose assuming compatibilization between the two materials. J Macromol Sci, Pure Appl Chem A33(12):1981–1996
Kachrimanis K, Malamataris S (2004) "Apparent" Young's elastic modulus and radial recovery for some tableted pharmaceutical excipients. Eur J Pharm Sci 21(2–3):197–207
Kaith BS, Singha AS, Dwivedi DK, Kumar S, Kumar D, Dhemeniya A (2003) Preparation of polystyrene matrix based composites using flax-g-copolymers as reinforcing agent and evaluation of their mechanical behaviour. Int J Plast Technol 7(2):119–125
Karmarkar A, Chauhan SS, Modak JM, Chanda M (2007) Mechanical properties of woodfiber reinforced polypropylene composites: effect of a novel compatibilizer with isocyanate functional group. Compos A 38(2):227–233
Kashiwagi T, Grulke E, Hilding J, Groth K, Harris R, Butler K, Shields J, Kharchenko S, Douglas J (2004) Thermal and flammability properties of polypropylene/carbon nanotube nanocomposites. Polymer 45(12):4227–4239
Kato K, Vasilets VN, Fursa MN, Meguro M, Ikada Y, Nakamae K (1999) Surface oxidation of cellulose fibers by vacuum ultraviolet irradiation. J Polym Sci, Part A: Polym Chem 37(3):357–361
Keller A (2003) Compounding and mechanical properties of biodegradable hemp fibre composites. Compos Sci Technol 63(9):1307–1316
Khan M, Haque N, Al-Kafi A, Alam MN, Abedin MZ (2006) Jute reinforced polymer composite by gamma radiation: effect of surface treatment with UV radiation. Polym Plast Technol Eng 45(5):607–613
Khan A, Khan RA, Salmieri S, Le Tien C, Riedl B, Bouchard J, Chauve G, Tan V, Kamal MR, Lacroix M (2012) Mechanical and barrier properties of nanocrystalline cellulose reinforced chitosan based nanocomposite films. Carbohydr Polym 90(4):1601–1608
Kiziltas A, Gardner DJ, Han Y, Yang H-S (2011a) Dynamic mechanical behavior and thermal properties of microcrystalline cellulose (MCC)-filled nylon 6 composites. Thermochim Acta 519(1–2):38–43
Kiziltas A, Gardner DJ, Han Y, Yang H-S (2011b) Thermal properties of microcrystalline cellulose-filled PET-PTT blend polymer composites. J Therm Anal Calorim 103(1):163–170
Kolar J, Strlic M, Müller-Hess D, Gruber A, Troschke K, Pentzien S, Kautek W (2000) Near-UV and visible pulsed laser interaction with paper. J Cult Herit 1:S221–S224
Kong K, Eichhorn SJ (2005) Crystalline and amorphous deformation of process-controlled cellulose-II fibres. Polymer 46(17):6380–6390
Krogars K, Heinamaki J, Vesalahti J, Marvola M, Antikainen O, Yliruusi J (2000) Extrusion-spheronization of pH-sensitive polymeric matrix pellets for possible colonic drug delivery. Int J Pharm 199(2):187–194
Krystynowicz A, Czaja W, Wiktorowska-Jezierska A, Goncalves-Miskiewicz M, Turkiewicz M, Bielecki S (2002) Factors affecting the yield and properties of bacterial cellulose. J Ind Microbiol Biotechnol 29(4):189–195
Kumar V, Medina MDLR, Leuenberger H (2005) Crosslinked powered/microfibrillated cellulose II as a pharmaceutical excipient. US Patent 2005287208
Kvien I, Sugiyama J, Votrubec M, Oksman K (2007) Characterization of starch based nanocomposites. J Mater Sci 42(19):8163–8171
Lahiji RR, Xu X, Reifenberger R, Raman A, Rudie A, Moon RJ (2010) Atomic force microscopy characterization of cellulose nanocrystals. Langmuir 26(6):4480–4488

Laka M, Chernyavskaya S, Maskavs M (2003) Cellulose-containing fillers for polymer composites. Mech Compos Mater 39(2):183–188

Lee SY, Kang IA, Doh GH, Yoon HG, Park BD (2008) Thermal and mechanical properties of wood flour/talc-filled polylactic acid composites: effect of filler content and coupling treatment. J Thermoplast Compos Mater 21(3):209–223

Lei Y, Wu Q, Yao F, Xu Y (2007) Preparation and properties of recycled HDPE/natural fiber composites. Compos A 38(7):1664–1674

Lenz J, Schurz J, Wrentschur E (1994) On the elongation mechanism of regenerated cellulose fibers. Holzforschung 48(Suppl.):72–76

Li F, Biagioni P, Finazzi M, Tavazzi S, Piergiovanni L (2013) Tunable green oxygen barrier through layer-by-layer self-assembly of chitosan and cellulose nanocrystals. Carbohydr Polym 92(2):2128–2134

Limwong V, Sutanthavibul N, Kulvanich P (2004) Spherical composite particles of rice starch and microcrystalline cellulose: a new coprocessed excipient for direct compression. AAPS PharmSciTech 5(2):e30

Lin N, Chen G, Huang J, Dufresne A, Chang PR (2009) Effects of polymer-grafted natural nanocrystals on the structure and mechanical properties of poly(lactic acid): a case of cellulose whisker-graft-polycaprolactone. J Appl Polym Sci 113(5):3417–3425

Ljungberg N, Bonini C, Bortolussi F, Boisson C, Heux L, Cavaille JY (2005) New nanocomposite materials reinforced with cellulose whiskers in atactic polypropylene: effect of surface and dispersion characteristics. Biomacromolecules 6(5):2732–2739

Ljungberg N, Cavaille JY, Heux L (2006) Nanocomposites of isotactic polypropylene reinforced with rod-like cellulose whiskers. Polymer 47(18):6285–6292

Lu JZ, Negulescu II, Wu Q (2005a) Maleated wood-fiber/high-density-polyethylene composites: coupling mechanisms and interfacial characterization. Compos Interfaces 12(1):125–140

Lu JZ, Wu Q, Negulescu II (2005b) Wood-fiber/high-density-polyethylene composites: coupling agent performance. J Appl Polym Sci 96(1):93–102

Lu W, Lin H, Chen G (2007) Voltage-induced resistivity relaxation in a high-density polyethylene/graphite nanosheet composite. J Polym Sci, Part B: Polym Phys 45(7):860–863

Lu J, Askeland P, Drzal LT (2008) Surface modification of microfibrillated cellulose for epoxy composite applications. Polymer 49(5):1285–1296

Luo H, Xiong G, Huang Y, He F, Wang Y, Wan Y (2008) Preparation and characterization of a novel COL/BC composite for potential tissue engineering scaffolds. Mater Chem Phys 110(2–3):193–196

Luukkonen P, Schaefer T, Hellen L, Juppo AM, Yliruusi J (1999) Rheological characterization of microcrystalline cellulose and silicified microcrystalline cellulose wet masses using a mixer torque rheometer. Int J Pharm 188(2):181–192

Ma H, Zhou B, Li H-S, Li Y-Q, Ou S-Y (2011) Green composite films composed of nanocrystalline cellulose and a cellulose matrix regenerated from functionalized ionic liquid solution. Carbohydr Polym 84(1):383–389

Maldas D, Kokta BV (1990) Effect of fiber treatment on the mechanical properties of hybrid fiber-reinforced polystyrene composites. I. Use of mica and wood pulp as hybrid filler. J Compos Technol Res 12(4):217–221

Maldas D, Kokta BV (1991a) Effect of fiber treatment on the mechanical properties of hybrid fiber reinforced polystyrene composites: IV. Use of glass fiber and sawdust as hybrid fiber. J Compos Mater 25(4):375–390

Maldas D, Kokta BV (1991b) Performance of treated hybrid fiber-reinforced thermoplastic composites under extreme conditions. IV. Use of glass fiber and sawdust as hybrid fiber. J Appl Polym Sci 42(5):1443–1450

Maldas D, Kokta BV (1991c) Performance of treated hybrid fiber-reinforced thermoplastic composites under extreme conditions: part I—use of mica and wood pulp as hybrid fiber. Polym Degrad Stab 31(1):9–21

Maldas D, Kokta BV (1992) Performance of hybrid reinforcements in PVC composites: III. Use of surface-modified glass fiber and wood pulp as reinforcements. J Reinf Plast Compos 11(10):1093–1102

Manchado MAL, Arroyo M, Biagiotti J, Kenny JM (2003) Enhancement of mechanical properties and interfacial adhesion of PP/EPDM/flax fiber composites using maleic anhydride as a compatibilizer. J Appl Polym Sci 90(8):2170–2178

Marchessault RH, Morehead FF, Walter NM (1959) Liquid crystal systems from fibrillar polysaccharides. Nature 184(Suppl. No. 9):632

Marins J, Soares B, Dahmouche K, Ribeiro SL, Barud H, Bonemer D (2011) Structure and properties of conducting bacterial cellulose-polyaniline nanocomposites. Cellulose 18(5):1285–1294

Mathew AP, Dufresne A (2002) Morphological investigation of nanocomposites from sorbitol plasticized starch and tunicin whiskers. Biomacromolecules 3(3):609–617

Mathew AP, Oksman K, Sain M (2005) Mechanical properties of biodegradable composites from poly lactic acid (PLA) and microcrystalline cellulose (MCC). J Appl Polym Sci 97(5):2014–2025

Mathew AP, Chakraborty A, Oksman K, Sain M (2006) The structure and mechanical properties of cellulose nanocomposites prepared by twin screw extrusion. In: Oksman K, Sain M (eds) Cellulose nanocomposites-processing, characterization and properties. American Chemical Society, Washington DC, p 114

Matsuda Y (2000) Properties and use of microfibrillated cellulose as papermaking additive. Sen'i Gakkaishi 56(7):192–196

Mehta G, Mohanty AK, Drzal LT, Misra M (2003) Bio-composites from engineered kenaf natural fibers and unsaturated polyester resin for low cost housing applications. PMSE Prepr 88:56–57

Millon LE, Wan WK (2006) The polyvinyl alcohol-bacterial cellulose system as a new nanocomposite for biomedical applications. J Biomed Mater Res B Appl Biomater 79B(2):245–253

Mirbagheri J, Tajvidi M, Hermanson JC, Ghasemi I (2007) Tensile properties of wood flour/kenaf fiber polypropylene hybrid composites. J Appl Polym Sci 105(5):3054–3059

Mizoguchi K, Ishikawa M, Ohkubo S, Yamamoto A, Ouchi A, Sakuragi M, Ito T, Sugiyama O (2001) Laser surface

treatment of regenerated cellulose fiber. Compos Interfaces 7(6):497–509

Mohanty AK, Misra M, Drzal LT (2001) Surface modifications of natural fibers and performance of the resulting biocomposites: an overview. Compos Interfaces 8(5):313–343

Nair KG, Dufresne A, Gandini A, Belgacem MN (2003) Crab shell chitin whiskers reinforced natural rubber nanocomposites. 3. Effect of chemical modification of chitin whiskers. Biomacromolecules 4(6):1835–1842

Nakagaito AN, Yano H (2004) Novel high-strength biocomposites based on microfibrillated cellulose having nano-order-unit web-like network structure. Appl Phys A Mater Sci Process 80(1):155–159

Nakagaito AN, Yano H (2008a) The effect of fiber content on the mechanical and thermal expansion properties of biocomposites based on microfibrillated cellulose. Cellulose 15(4):555–559

Nakagaito AN, Yano H (2008b) Toughness enhancement of cellulose nanocomposites by alkali treatment of the reinforcing cellulose nanofibers. Cellulose 15(2):323–331

Nakagaito AN, Iwamoto S, Yano H (2005) Bacterial cellulose: the ultimate nano-scalar cellulose morphology for the production of high-strength composites. Appl Phys A Mater Sci Process 80(1):93–97

Nishi Y, Uryu M, Yamanaka S, Watanabe K, Kitamura N, Iguchi M, Mitsuhashi S (1990) The structure and mechanical properties of sheets prepared from bacterial cellulose. Part 2. Improvement of the mechanical properties of sheets and their applicability to diaphragms of electroacoustic transducers. J Mater Sci 25(6):2997–3001

Nishino T, Arimoto N (2007) All-cellulose composite prepared by selective dissolving of fiber surface. Biomacromolecules 8(9):2712–2716

Nishino T, Hirao K, Kotera M, Nakamae K, Inagaki H (2003) Kenaf reinforced biodegradable composite. Compos Sci Technol 63(9):1281–1286

Nishino T, Matsuda I, Hirao K (2004) All-cellulose composite. Macromolecules 37(20):7683–7687

Nishiyama S, Funato N, Sawatari A (1993) Analysis of the functional groups formed on the corona-treated cellulose fiber sheet surface by chemical modification in gas-phase ESCA technique. Sen'i Gakkaishi 49(7):357–366

Njuguna J, Pielichowski K, Alcock JR (2007) Epoxy-based fibre reinforced nanocomposites. Adv Eng Mater 9(10):835–847

Nourbakhsh A, Ashori A (2008) Fundamental studies on wood-plastic composites: effects of fiber concentration and mixing temperature on the mechanical properties of poplar/PP composite. Polym Compos 29(5):569

Oksman K, Mathew AP, Bondeson D, Kvien I (2006) Manufacturing process of cellulose whiskers/polylactic acid nanocomposites. Compos Sci Technol 66(15):2776–2784

Oliveira Taipina M, Ferrarezi M, Yoshida IVP, Gonçalves Md (2013) Surface modification of cotton nanocrystals with a silane agent. Cellulose 20(1):217–226

Ouali N, Cavaille JY, Perez J (1991) Elastic, viscoelastic and plastic behavior of multiphase polymer blends. Plast Rubber Compos Process Appl 16(1):55–60

Page DH (1969) Theory for the tensile strength of paper. Tappi 52(4):674–681

Page DH, El-Hosseiny F, Winkler K (1971) Behaviour of single wood fibres under axial tensile strain. Nature 229:252–253

Pan P, Zhu B, Dong T, Serizawa S, Iji M, Inoue Y (2008) Kenaf fiber/poly(e-caprolactone) biocomposite with enhanced crystallization rate and mechanical properties. J Appl Polym Sci 107(6):3512–3519

Panshin AJ, de Zeeuw C (1980) Textbook of wood technology: structure, identification, properties, and uses of the commercial woods of the United States and Canada. McGraw-Hill, New York, NY

Pei A, Malho J-M, Ruokolainen J, Zhou Q, Berglund LA (2011) Strong nanocomposite reinforcement effects in polyurethane elastomer with low volume fraction of cellulose nanocrystals. Macromolecules 44(11):4422–4427

Petersson L, Oksman K (2006) Preparation and properties of biopolymer-based nanocomposite films using microcrystalline cellulose. In: Oksman K, Sain M (eds) Cellulose nanocomposites-processing, characterization and properties. American Chemistry Society, Washington DC, p 132

Petersson L, Kvien I, Oksman K (2007) Structure and thermal properties of poly(lactic acid)/cellulose whiskers nanocomposite materials. Compos Sci Technol 67(11–12):2535–2544

Phiriyawirut M, Saenpong P, Chalermboon S, Sooksakoolrut R, Pochanajit N, Vuttikit L, Thongchai A, Supaphol P (2008) Isotactic poly(propylene)/wood sawdust composite: effects of natural weathering, water immersion, and gamma-ray irradiation on mechanical properties. Macromol Symp 264(1):59–66

Pullawan T, Wilkinson AN, Eichhorn SJ (2010) Discrimination of matrix-fibre interactions in all-cellulose nanocomposites. Compos Sci Technol 70(16):2325–2330

Pullawan T, Wilkinson AN, Eichhorn SJ (2012) Influence of magnetic field alignment of cellulose whiskers on the mechanics of all-cellulose nanocomposites. Biomacromolecules 13(8):2528–2536

Qi H, Cai J, Zhang L, Kuga S (2009) Properties of films composed of cellulose nanowhiskers and a cellulose matrix regenerated from alkali/urea solution. Biomacromolecules 10(6):1597–1602

Qin C, Soykeabkaew N, Xiuyuan N, Peijs T (2008) The effect of fibre volume fraction and mercerization on the properties of all-cellulose composites. Carbohydr Polym 71(3):458–467

Qiu K, Netravali AN (2012) Fabrication and characterization of biodegradable composites based on microfibrillated cellulose and polyvinyl alcohol. Compos Sci Technol 72(13):1588–1594

Quillin DT, Caulfield DF, Koutsky JA (1992) Surface energy compatibilities of cellulose and polypropylene. Mater Res Soc Symp Proc 266:113–126

Quillin DT, Caufield DF, Koutsky JA (1993) Crystallinity in the polypropylene/cellulose system. I. Nucleation and crystalline morphology. J Appl Polym Sci 50(7):1187–1194

Quillin DT, Yin M, Koutsky JA, Caulfield DF (1994) Crystallinity in the polypropylene/cellulose system. II. Crystallization kinetics. J Appl Polym Sci 52(5):605–615

Radovanovic B, Markovic G, Radovanovic A (2008) Wood flour as a secondary filler in carbon black filled of styrene butadiene/chlorosulphonated polyethylene rubber blend. Polym Compos 29(6):692–697

Rånby BG (1951) The colloidal properties of cellulose micelles. Discuss Faraday Soc 11:158–164 (discussion 208–113)

Rånby BG (1952) The cellular micelles. Tappi 35:53–58
Ray PK, Chakravarty AC, Bandyopadhyay SB (1976) Fine structure and mechanical properties of jute differently dried after retting. J Appl Polym Sci 20(7):1765–1767
Report (2002) Annual report of the government-industry forum on non-food uses of crops. Department for Environment, Food and Rural Affairs, EU
Retegi A, Algar I, Martin L, Altuna F, Stefani P, Zuluaga R, Gañán P, Mondragon I (2012) Sustainable optically transparent composites based on epoxidized soy-bean oil (ESO) matrix and high contents of bacterial cellulose (BC). Cellulose 19(1):103–109
Revol JF, Bradford H, Giasson J, Marchessault RH, Gray DG (1992) Helicoidal self-ordering of cellulose microfibrils in aqueous suspension. Int J Biol Macromol 14(3):170–172
Revol JF, Godbout L, Dong XM, Gray DG, Chanzy H, Maret G (1994) Chiral nematic suspensions of cellulose crystallites; phase separation and magnetic field orientation. Liq Cryst 16(1):127–134
Revol JF, Godbout L, Gray DG (1998) Solid self-assembled films of cellulose with chiral nematic order and optically variable properties. J Pulp Pap Sci 24(5):146–149
Rezaei F, Yunus R, Ibrahim NA, Mahdi ES (2008) Development of short-carbon-fiber-reinforced polypropylene composite for car bonnet. Polym Plast Technol Eng 47(4):351–357
Rodionova G, Lenes M, Eriksen Ø, Gregersen Ø (2011) Surface chemical modification of microfibrillated cellulose: improvement of barrier properties for packaging applications. Cellulose 18(1):127–134
Roman M, Winter WT (2004) Effect of sulfate groups from sulfuric acid hydrolysis on the thermal degradation behavior of bacterial cellulose. Biomacromolecules 5(5): 1671–1677
Ruiz MM, Cavaille JY, Dufresne A, Graillat C, Gerard J-F (2001) New waterborne epoxy coatings based on cellulose nanofillers. Macromol Symp 169(1):211–222
Sabharwal HS, Denes F, Nielsen L, Young RA (1993) Free-radical formation in jute from argon plasma treatment. J Agric Food Chem 41(11):2202–2207
Saechtling H (1987) Saechtling international plastics handbook for the technologist, engineer, and user. Carl Hanser Verlag, Munich
Sahoo PK, Sahu GC, Rana PK, Das AK (2005) Preparation, characterization, and biodegradability of jute-based natural fiber composite superabsorbents. Adv Polym Technol 24(3):208–214
Saito T, Nishiyama Y, Putaux J-L, Vignon M, Isogai A (2006) Homogeneous suspensions of individualized microfibrils from TEMPO-catalyzed oxidation of native cellulose. Biomacromolecules 7(6):1687–1691
Saito T, Kuramae R, Wohlert J, Berglund LA, Isogai A (2013) An ultrastrong nanofibrillar biomaterial: the strength of single cellulose nanofibrils revealed via sonication-induced fragmentation. Biomacromolecules 14(1):248–253
Sakamoto A (2008) Sauce compositions containing stabilizers. JP Patent 2008271879
Sakurada I, Nukushina Y (1962) Experimental determination of the elastic modulus of crystalline regions in oriented polymers. J Polym Sci 57(165):651–660
Samir MASA, Alloin F, Sanchez J-Y, Dufresne A (2004a) Cross-linked nanocomposite polymer electrolytes reinforced with cellulose whiskers. Macromolecules 37(13):4839–4844
Samir MASA, Alloin F, Sanchez J-Y, El Kissi N, Dufresne A (2004b) Preparation of cellulose whiskers reinforced nanocomposites from an organic medium suspension. Macromolecules 37(4):1386–1393
Samir MASA, Alloin F, Sanchez J-Y, Dufresne A (2004c) Cellulose nanocrystals reinforced poly(oxyethylene). Polymer 45(12):4149–4157
Samir MASA, Alloin F, Dufresne A (2005a) Review of recent research into cellulosic whiskers, their properties and their application in nanocomposite field. Biomacromolecules 6(2):612–626
Samir MASA, Alloin F, Sanchez J-Y, Dufresne A (2005b) Nanocomposite polymer electrolytes based on poly(oxyethylene) and cellulose whiskers. Polim Cienc Tecnol 15(2):109–113
Sarkhel G, Choudhury A (2008) Dynamic mechanical and thermal properties of PE-EPDM based jute fiber composites. J Appl Polym Sci 108(6):3442–3453
Sawatari A, Nakamura H (1993) Surface characterization of the corona-treated cellulose fiber sheet by chemical modification—ESCA technique. (Part 1). Analysis of the functional groups formed on the corona-treated cellulose fiber sheet surface by means of chemical modification in liquid phase-ESCA technique. Sen'i Gakkaishi 49(6):279–286
Seidel A (ed) (2004) Kirk-Othmer encyclopedia of chemical technology, vol 5, 5th edn. Wiley-Interscience, Hoboken
Semsarzadeh MA (1986) Fiber matrix interactions in jute reinforced polyester resin. Polym Compos 7(1):23–25
Setua DK, De SK (1984) Short silk fibre reinforced nitrile rubber composites. J Mater Sci 19(3):983–999
Shah J, Brown Jr. RM (2005) Towards electronic paper displays made from microbial cellulose. Appl Microbiol Biotechnol 66(4):352
Shang W, Huang J, Luo H, Chang P, Feng J, Xie G (2013) Hydrophobic modification of cellulose nanocrystal via covalently grafting of castor oil. Cellulose 20(1):179–190
Singh S, Mohanty AK (2007) Wood fiber reinforced bacterial bioplastic composites: fabrication and performance evaluation. Compos Sci Technol 67(9):1753–1763
Singh S, Mohanty AK, Sugie T, Takai Y, Hamada H (2008) Renewable resource based biocomposites from natural fiber and polyhydroxybutyrate-co-valerate (PHBV) bioplastic. Compos A 39(5):875–886
Siró I, Plackett D (2010) Microfibrillated cellulose and new nanocomposite materials: a review. Cellulose 17(3): 459–494
Soykeabkaew N, Arimoto N, Nishino T, Peijs T (2008) All-cellulose composites by surface selective dissolution of aligned ligno-cellulosic fibres. Compos Sci Technol 68(10–11): 2201–2207
Spence K, Venditti R, Rojas O, Habibi Y, Pawlak J (2010) The effect of chemical composition on microfibrillar cellulose films from wood pulps: water interactions and physical properties for packaging applications. Cellulose 17(4):835–848
Spence K, Venditti R, Rojas O, Habibi Y, Pawlak J (2011a) A comparative study of energy consumption and physical properties of microfibrillated cellulose produced by different processing methods. Cellulose 18(4):1097–1111

Spence K, Venditti R, Rojas O, Pawlak J, Hubbe M (2011b) Water vapor barrier properties of coated and filled microfibrillated cellulose composite films. BioRes 6(4):4370–4388

Sretenovic A, Muller U, Gindl W (2006) Mechanism of stress transfer in a single wood fibre-LDPE composite by means of electronic laser speckle interferometry. Compos A 37(9): 1406–1412

Srithep Y, Turng L-S, Sabo R, Clemons C (2012) Nanofibrillated cellulose (NFC) reinforced polyvinyl alcohol (PVOH) nanocomposites: properties, solubility of carbon dioxide, and foaming. Cellulose 19(4):1209–1223

Stauffer D (1985) Introduction to percolation theory. Talor and Francis, London

Šturcová A, Davies GR, Eichhorn SJ (2005) Elastic modulus and stress-transfer properties of tunicate cellulose whiskers. Biomacromolecules 6(2):1055–1061

Suddell BC, Evans WJ (2003) The increasing use and application of natural fiber composite materials within the automotive industry. In: Seventh international conference on woodfiber-plastic composites, Madison, Wisconsin, USA, pp 7–14

Suddell BC, Evans WJ (2005) Natural fiber composites in automotive applications. In: Mohanty AK, Misra M, Drzal LT (eds) Natural fibers, biopolymers and biocomposites. CRC, USA

Sundar S, Sain M, Oksman K (2011) Thermal characterization and electrical properties of Fe-modified cellulose long fibers and micro crystalline cellulose. J Therm Anal Calorim 104(3):841–847

Swatloski RP, Spear SK, Holbrey JD, Rogers RD (2002) Dissolution of cellose with ionic liquids. J Am Chem Soc 124(18):4974–4975

Swatloski RP, Holbrey JD, Rogers RD (2003) Ionic liquids are not always green: hydrolysis of 1-butyl-3-methylimidazolium hexafluorophosphate. Green Chem 5(4):361–363

Tajvidi M (2005) Static and dynamic mechanical properties of a kenaf fiber-wood flour/polypropylene hybrid composite. J Appl Polym Sci 98(2):665–672

Takacs E, Wojnarovits L, Borsa J, Foldvary C, Hargittai P, Zold O (1999) Effect of gamma-irradiation on cotton-cellulose. Radiat Phys Chem 55(5–6):663–666

Taniguchi T, Okamura K (1998) New films produced from microfibrillated natural fibers. Polym Int 47(3):291–294

Tanpichai S, Quero F, Nogi M, Yano H, Young RJ, Lindström T, Sampson WW, Eichhorn SJ (2012a) Effective Young's modulus of bacterial and microfibrillated cellulose fibrils in fibrous networks. Biomacromolecules 13(5):1340–1349

Tanpichai S, Sampson WW, Eichhorn SJ (2012b) Stress-transfer in microfibrillated cellulose reinforced poly(lactic acid) composites using Raman spectroscopy. Compos A 43(7): 1145–1152

Thummanukitcharoen P, Limpanart S, Srikulkit K (2012) Preparation of organosilane treated microcrystalline (SiMCC) and SiMCC/polypropylene composites. J Metals Mater Miner 22(1):13–19

Thuy Pham TP, Cho C-W, Yun Y-S (2010) Environmental fate and toxicity of ionic liquids: a review. Water Res 44(2):352–372

Thwe MM, Liao K (2000) Characterization of bamboo-glass fiber reinforced polymer matrix hybrid composite. J Mater Sci Lett 19(20):1873–1876

Thwe MM, Liao K (2003) Environmental effects on bamboo-glass/polypropylene hybrid composites. J Mater Sci 38(2): 363–376

Thygesen A, Daniel G, Lilholt H, Thomsen AB (2005) Hemp fiber microstructure and use of fungal defibration to obtain fibers for composite materials. J Nat Fibers 2(4):19–37

Trejo-O'Reilly JA, Cavaille JY, Paillet M, Gandini A, Herrera-Franco P, Cauich J (2000) Interfacial properties of regenerated cellulose fiber/polystyrene composite materials. Effect of the coupling agent's structure on the micromechanical behavior. Polym Compos 21(1):65–71

Tsai SW, Halpin JC, Pagano NJ (1968) Composite materials workshop. Technomic Publishing Co., New York

Turbak AF, El-Kafrawy A, Snyder FW Jr, Auerbach AB (1981) Solvent system for celulose. US Patent 4302252

Turbak AF, Snyder FW, Sandberg KR (1983) Microfibrillated cellulose, a new cellulose product: properties, uses, and commercial potential. J Appl Polym Sci: Appl Polym Symp 37:815–827

Uehara T, Sakata I (1990) Effect of corona discharge treatment on cellulose prepared from beechwood. J Appl Polym Sci 41(7–8):1695–1706

Ummartyotin S, Juntaro J, Sain M, Manuspiya H (2012) Development of transparent bacterial cellulose nanocomposite film as substrate for flexible organic light emitting diode (OLED) display. Ind Crops Prod 35(1):92–97

Urabe K, Yomoda S (1991) A nondestructive testing method of fiber orientation by microwave. Adv Compos Mater 1(3): 193–208

Vallejos ME, Peresin MS, Rojas OJ (2012) All-cellulose composite fibers obtained by electrospinning dispersions of cellulose acetate and cellulose nanocrystals. J Polym Environ 20(4):1075–1083

van den Berg O, Capadona JR, Weder C (2007) Preparation of homogeneous dispersions of tunicate cellulose whiskers in organic solvents. Biomacromolecules 8(4):1353–1357

Vilay V, Mariatti M, Mat Taib R, Todo M (2008) Effect of fiber surface treatment and fiber loading on the properties of bagasse fiber-reinforced unsaturated polyester composites. Compos Sci Technol 68(3–4):631–638

Wang Y, Chen L (2011) Impacts of nanowhisker on formation kinetics and properties of all-cellulose composite gels. Carbohydr Polym 83(4):1937–1946

Wang N, Ding E, Cheng R (2007) Thermal degradation behaviors of spherical cellulose nanocrystals with sulfate groups. Polymer 48(12):3486–3493

Westerlind B, Larsson A, Rigdahl M (1987) Determination of the degree of adhesion in plasma-treated polyethylene/paper laminates. Int J Adhes Adhes 7(3):141–146

Whiteside BR, Coates PD, Hine PJ, Duckett RA (2000) Glass fibre orientation within injection moulded automotive pedal simulation and experimental studies. Plast, Rubber Compos 29(1):38–45

Wu Q, Henriksson M, Liu X, Berglund LA (2007) A high strength nanocomposite based on microcrystalline cellulose and polyurethane. Biomacromolecules 8(12):3687–3692

Xiang C, Taylor AG, Hinestroza JP, Frey MW (2013) Controlled release of nonionic compounds from poly(lactic acid)/cellulose nanocrystal nanocomposite fibers. J Appl Polym Sci 127(1):79–86

Xiao L, Mai Y, He F, Yu L, Zhang L, Tang H, Yang G (2012) Bio-based green composites with high performance from poly(lactic acid) and surface-modified microcrystalline cellulose. J Mater Chem 22(31):15732–15739

Yamanaka S, Watanabe K, Kitamura N, Iguchi M, Mitsuhashi S, Nishi Y, Uryu M (1989) The structure and mechanical properties of sheets prepared from bacterial cellulose. J Mater Sci 24(9):3141–3145

Yang Q, Lue A, Zhang L (2010) Reinforcement of ramie fibers on regenerated cellulose films. Compos Sci Technol 70(16): 2319–2324

Yang H-S, Gardner DJ, Nader JW (2011) Dispersion evaluation of microcrystalline cellulose/cellulose nanofibril-filled polypropylene composites using thermogravimetric analysis. J Therm Anal Calorim 103(3):1007–1015

Yang J, Han C-R, Duan J-F, Ma M-G, Zhang X-M, Xu F, Sun R-C, Xie X-M (2012) Studies on the properties and formation mechanism of flexible nanocomposite hydrogels from cellulose nanocrystals and poly(acrylic acid). J Mater Chem 22(42):22467–22480

Yang J, Han C-R, Duan J-F, Ma M-G, Zhang X-M, Xu F, Sun R-C (2013) Synthesis and characterization of mechanically flexible and tough cellulose nanocrystals-polyacrylamide nanocomposite hydrogels. Cellulose 20(1):227–237

Yano H, Sugiyama J, Nakagaito AN, Nogi M, Matsuura T, Hikita M, Handa K (2005) Optically transparent composites reinforced with networks of bacterial nanofibers. Adv Mater 17(2):153–155

Young Christopher R, Koleng John J, McGinity James W (2002) Production of spherical pellets by a hot-melt extrusion and spheronization process. Int J Pharm 242(1–2):87–92

Yousefi H, Faezipour M, Nishino T, Shakeri A, Ebrahimi G (2011a) All-cellulose composite and nanocomposite made from partially dissolved micro- and nanofibers of canola straw. Polym J 43(6):559–564

Yousefi H, Nishino T, Faezipour M, Ebrahimi G, Shakeri A (2011b) Direct fabrication of all-cellulose nanocomposite from cellulose microfibers using ionic liquid-based nanowelding. Biomacromolecules 12(11):4080–4085

Yuan H, Nishiyama Y, Wada M, Kuga S (2006) Surface acylation of cellulose whiskers by drying aqueous emulsion. Biomacromolecules 7(3):696–700

Yuan Q, Wu D, Gotama J, Bateman S (2008) Wood fiber reinforced polyethylene and polypropylene composites with high modulus and impact strength. J Thermoplast Compos Mater 21(3):195–208

Zarate CN, Aranguren MI, Reboredo MM (2008) Thermal degradation of a phenolic resin, vegetable fibers, and derived composites. J Appl Polym Sci 107(5):2977–2985

Zeronian SH (1991) The mechanical properties of cotton fibers. J Appl Polym Sci: Appl Polym Symp 47:445–461

Zeronian SH, Kawabata H, Alger KW (1990) Factors affecting the tensile properties of nonmercerized and mercerized cotton fibers. Text Res J 60(3):179–183

Zhang X, Shen J, Yang H, Lin Z, Tan S (2011) Mechanical properties, morphology, thermal performance, crystallization behavior, and kinetics of PP/microcrystal cellulose composites compatibilized by two different compatibilizers. J Thermoplast Compos Mater 24(6):735–754

Zhao Q, Yam RM, Zhang B, Yang Y, Cheng X, Li RY (2009) Novel all-cellulose ecocomposites prepared in ionic liquids. Cellulose 16(2):217–226

Zhou Y, Pervin F, Rangari VK, Jeelani S (2006) Fabrication and evaluation of carbon nanofiber filled carbon/epoxy composite. Mater Sci Eng, A 426(1–2):221–228

Zhou C, Chu R, Wu R, Wu Q (2011a) Electrospun polyethylene oxide/cellulose nanocrystal composite nanofibrous mats with homogeneous and heterogeneous microstructures. Biomacromolecules 12(7):2617–2625

Zhou C, Wu Q, Yue Y, Zhang Q (2011b) Application of rod-shaped cellulose nanocrystals in polyacrylamide hydrogels. J Colloid Interface Sci 353(1):116–123

Zimmerman JM, Losure NS (1998) Mechanical properties of kenaf bast fiber reinforced epoxy matrix composite panels. J Adv Mater 30(2):32–38